

# Spontaneous emission from a three-level atom embedded in an anisotropic photonic crystal

 S.-y. Xie<sup>1,a</sup>, Y.-p. Yang<sup>1,2</sup>, and X. Wu<sup>1</sup>
<sup>1</sup> Department of Physics, Tongji University, 1239 Sipin road, Shanghai 200092, P.R. China

<sup>2</sup> Department of Physics, Hongkong Baptist University, Hong Kong

Received 9 April 2000 and Received in final form 1st August 2000

**Abstract.** We study the spontaneous emission properties of a V-type three-level atom embedded in a photonic crystal with the anisotropic dispersion relation. We show that the localized field can disappear and the diffusion field can become intense in some regions. This originates from no singularity of the density of states. The quantum interference leads to oscillatory, quasi-oscillatory or complete decay behavior of population. The complete decay can also be realized in certain condition without depending on the initial state.

**PACS.** 42.70.Qs Photonic bandgap materials – 42.50.Dv Nonclassical field states; squeezed, antibunched, and sub-Poissonian states; operational definitions of the phase of the field; phase measurements – 32.80.Bx Level crossing and optical pumping

## 1 Introduction

Photonic crystals are artificially created three-dimensional periodic dielectric structures [1–3] with the existence of one or several full photonic band gaps (PBG). The propagation of electromagnetic (EM) waves with frequencies within the gaps is forbidden in all directions, similar to the case of electron waves propagating in a crystal. The periodic dielectric structures make the dispersion relation in photonic crystals different strongly from that in vacuum. The density of states (DOS) varies rapidly with frequency in a manner determined by the photon dispersion relation,  $\omega_k$ . The electromagnetic field mode density in photonic crystals is deformed due to the modification of the dispersion relation. The properties of photonic crystals provides a way to control spontaneous emission of the excited atom [4–10], which would promote the development of optics and optoelectronics, and has many important applications [3]. The previous studies show that the gap edge has great influences on optical behavior of an atom in a photonic crystal, and many interesting effects have been predicted when radiative transitions of the atoms are near resonant with the photonic band edge, such as suppression and even complete cancellation of spontaneous emission, the formation of photon-atom bound states [4, 6–8], spectral splitting [5, 8], periodic and quasiperiodic oscillations, enhancement of spontaneous emission interference [8], coherent control of spontaneous emission [10], non-exponential spontaneous emission [4, 6] etc.

Many earlier studies are based on the isotropic model, and the photon dispersion relation  $\omega_k$  near the band edge was assumed to be isotropic [4–10] and described by  $\omega_k = \omega_c + A(k - k_0)^2$ . This assumption is not suitable as for the real photonic crystals because a real photonic crystal in general has an anisotropic structure in the momentum space (relation of  $\omega$  over  $k$ ), and a three-dimensional anisotropic dispersion relation is required. For a real three-dimensional photonic crystal with an allowed point-group symmetry, the band edge is associated with a specific point  $\mathbf{k} = \mathbf{k}_0$  or a finite collection of symmetry related points rather than the entire sphere  $|\mathbf{k}| = |\mathbf{k}_0|$ . For example, the collection of symmetry points  $\mathbf{k}_0^n$  are the eight  $L$  points on the surface of the first Brillouin zone (BZ) of a diamond photonic crystal structure. Although the isotropic dispersion relation is formally simple, it overestimates the effects of the band edge because the isotropic dispersion relation represents that the band edge can appear on the surface of the entire sphere  $|\mathbf{k}| = |\mathbf{k}_0|$ . The great difference between anisotropic and isotropic photonic crystals stems from the dependence of density of state (DOS) on the band edge. As for the three-dimensional case with anisotropic dispersion relation, the density of state is proportional to  $(\omega_k - \omega_c)^{1/2}$  for  $(\omega_k > \omega_c)$  ( $\omega_k$  is the frequency of the  $k$ th vacuum mode) which is not singular. In contrast, for an isotropic band gap structure with isotropic dispersion relation, the density of state is proportional to  $(\omega_k - \omega_c)^{-1/2}$  for  $(\omega_k > \omega_c)$ , which leads to a singularity at the band edge. In a recent paper on spontaneous emission from a two-level atom in a photonic crystal with anisotropic dispersion relation, some novel properties are

---

<sup>a</sup> e-mail: xieshy@hotmail.com or xieshy@baoscape.com

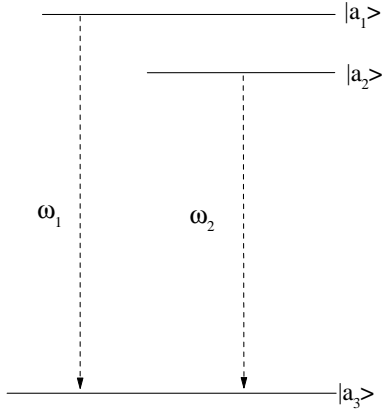


**Fig. 1.** The scheme of the three-level atom in this system.

shown [11]. We predict that the difference of the density of states can also significantly change the properties of the spontaneous emission from a three-level atom because the density of states plays an important role in the interaction between light and materials.

In this paper, we investigate the spontaneous emission from a V-type three-level atom embedded in a three-dimensional photonic crystal when the anisotropic dispersion relation is taken into account. We found the significant difference between the isotropic and anisotropic models resulting from the difference of the DOS. The localized field can disappear and the diffusion field can become intense in some regions. The population displays oscillatory, quasi-oscillatory or complete decay behaviors because of the quantum interference. The complete decay can be realized with any initial state in certain condition.

This paper is outlined as follows: in next section we present the model and the basic theory to study the spontaneous emission; in Section 3, we investigate the properties of the emitted field in detail. The properties of the population trapped in the excited state are discussed in Section 4.

## 2 The model and the basic theory

We consider a three-level atom with two upper levels  $|a_1\rangle$ ,  $|a_2\rangle$  and a lower level  $|a_3\rangle$  (as shown in Fig. 1) embedded in an anisotropic photonic crystal. The two upper levels  $|a_1\rangle$ ,  $|a_2\rangle$  are coupled by the same vacuum modes to the ground level  $|a_3\rangle$ . The resonant transition frequencies between levels  $|a_1\rangle$ ,  $|a_2\rangle$  and  $|a_3\rangle$  are, respectively,  $\omega_1$  and  $\omega_2$ , which are assumed to be near the band edge. The energy of the lower level  $|a_3\rangle$  is set to be zero. Near the band edge of the three-dimensional photonic crystal,  $\omega_c$ , the dispersion relation for the  $\mathbf{k}$  whose directions are near one of  $\mathbf{k}_0^n$  ( $n = 1, 2 \dots 8$ ) could be expressed approximately as:

$$\omega_k = \omega_c + A|\mathbf{k} - \mathbf{k}_0^n|^2 \quad (1)$$

where  $\omega_c$  is the cut-off frequency of the corresponding band edge, and  $A$  is a model dependent constant. The band edge DOS corresponding to equation (1) takes the form  $\rho(\omega) \sim (\omega - \omega_c)^{1/2}$  for  $\omega > \omega_c$ .

Performing the rotating wave approximation (RWA) for the interaction term, the second quantized Hamiltonian for the system under consideration takes the form:

$$\hat{H} = \sum_{j=1,2} \hbar\omega_j |a_j\rangle\langle a_j| + \sum_k \hbar\omega_k b_k^\dagger b_k + i\hbar \sum_k \sum_{j=1,2} \left[ g_k^{(j)} b_k^\dagger |a_3\rangle\langle a_j| - \text{h.c.} \right] \quad (2)$$

where  $b_k$  ( $b_k^\dagger$ ) is the radiation field annihilation (creation) operator for the  $k$ th electromagnetic mode with frequency  $\omega_k$ . The coupling constants between the  $k$ th electromagnetic mode and the atomic transitions  $|a_j\rangle \rightarrow |a_3\rangle$  ( $j = 1, 2$ ) are  $g_k^{(j)} = (\omega_j d_j / \hbar) (\hbar / 2\epsilon_0 \omega_k V_0)^{1/2} \mathbf{e}_k \cdot \mathbf{u}_j$ , which are assumed to be real.  $k$  represents both the momentum and polarization of the radiation modes.  $d_j$  and  $\mathbf{u}_j$  are the magnitude and unit vector of the atomic dipole moment of the transitions,  $V_0$  is the quantization volume,  $\mathbf{e}_k$  are the two transverse unit vectors, and  $\epsilon_0$  is the Coulomb constant.

The state vector of the system at any time  $t$  can be written as:

$$|\Psi(t)\rangle = \sum_{j=1,2} A_j(t) e^{-i\omega_j t} |a_j\rangle |0\rangle_f + \sum_k B_k(t) e^{-i\omega_k t} |a_3\rangle |1_k\rangle_f, \quad (3)$$

where the state vectors  $|a_j\rangle |0\rangle_f$  ( $j = 1, 2$ ) describe the atom in its excited states  $|a_j\rangle$  and no photons are present in reservoir modes, and the state vector  $|a_3\rangle |1_k\rangle_f$  describes the atom in its ground state  $|a_3\rangle$  with a single photon in  $k$ th mode with frequency  $\omega_k$ . We assume the atom initially to be excited, *i.e.*  $|A_1(0)|^2 + |A_2(0)|^2 = 1$  and  $B_k(0) = 0$ . Substituting equations (2), (3) into the Schrödinger equation, we can obtain the following equations about the amplitudes  $A_1(t)$ ,  $A_2(t)$  and  $B_k(t)$ :

$$\begin{aligned} \frac{\partial}{\partial t} A_1(t) &= - \sum_k g_k^{(1)} B_k(t) e^{-i(\omega_k - \omega_1)t}, \\ \frac{\partial}{\partial t} A_2(t) &= - \sum_k g_k^{(2)} B_k(t) e^{-i(\omega_k - \omega_2)t}, \\ \frac{\partial}{\partial t} B_k(t) &= g_k^{(1)} A_1(t) e^{i(\omega_k - \omega_1)t} + g_k^{(2)} A_2(t) e^{i(\omega_k - \omega_2)t}. \end{aligned} \quad (4)$$

Formally integrating the third equation in equations (4) and substituting it into the preceding two equations, we use the Laplace transform to get the Laplace transforms  $A_{1,2}(s)$  for the amplitudes  $A_{1,2}(t)$ :

$$\begin{aligned} A_1(s) &= \frac{A_1(0)(s - i\omega_{12} + \Gamma_{22}) - A_2(0)\Gamma_{12}}{(s + \Gamma_{11})(s - i\omega_{12} + \Gamma_{22}) - (\Gamma_{12})^2}, \\ A_2(s - i\omega_{12}) &= \frac{A_2(0)(s + \Gamma_{11}) - A_1(0)\Gamma_{12}}{(s + \Gamma_{11})(s - i\omega_{12} + \Gamma_{22}) - (\Gamma_{12})^2} \end{aligned} \quad (5)$$

where  $\Gamma_{lm} = \sum_k g_k^{(l)} g_k^{(m)} / (s - i(\omega_1 - \omega_k))$  ( $l, m = 1, 2$ ),  $\omega_{12} = \omega_1 - \omega_2$ . In the following discussion, we consider the atomic dipole moments of the two transitions  $|a_i\rangle \rightarrow |a_3\rangle$

( $i = 1, 2$ ) are parallel to each other. Using the dispersion relation equation (1), we can obtain

$$\begin{aligned}\Gamma_{11} &= -i\beta_1^{3/2}/(\sqrt{\omega_c} + \sqrt{-is - \omega_{1c}}), \\ \Gamma_{22} &= -i\beta_2^{3/2}/(\sqrt{\omega_c} + \sqrt{-is - \omega_{1c}}), \\ \text{and } \Gamma_{12} &= -i(\beta_1\beta_2)^{3/4}/(\sqrt{\omega_c} + \sqrt{-is - \omega_{1c}})\end{aligned}$$

with  $\omega_{1c} = \omega_1 - \omega_c$ ,  $\omega_{2c} = \omega_2 - \omega_c$ , and

$$\beta_j^{3/2} = \left[ \frac{(\omega_j d_j)^2}{8\pi\epsilon_0 \hbar A^{3/2}} \left( \sum_n \sin^2 \theta_n \right) \right],$$

( $j = 1, 2$ ) (see Appendix A).  $\theta_n$  is the angle between the dipole vector of the atom and  $\mathbf{k}_0^n$ . In deriving  $\Gamma$ , the summation over  $\mathbf{k}$  was replaced by an integration over  $\mathbf{k}$ , and the variables of integration was changed to  $\mathbf{q} = \mathbf{k} - \mathbf{k}_0^n$ . Due to the anisotropy in three-dimensional photonic crystals, both the direction and magnitude of the band edge wavevector are modified as  $\mathbf{k}$  moves away from  $\mathbf{k}_0^n$ . So the integration over  $\mathbf{k}$  has to be carried out around the directions of each  $\mathbf{k}_0^n$ , respectively. For the sake of simplicity, we assume  $g_k^{(1)} = g_k^{(2)} = g_k$ , and we have  $\beta_1^{3/2} = \beta_2^{3/2} = \beta^{3/2}$ ,  $\Gamma_{11} = \Gamma_{22} = \Gamma_{12} = \Gamma$ . At this point, it should be stressed that the phase angle of  $\sqrt{-is - \omega_{1c}}$  in  $\Gamma$  has been defined as  $-\pi/2 < \arg(\sqrt{-is - \omega_{1c}}) < \pi/2$ .

The amplitudes  $A_1(t)$ ,  $A_2(t)$  can be calculated by means of the inverse Laplace transform

$$\begin{aligned}A_1(t) &= \frac{1}{2\pi i} \int_{\sigma-i\infty}^{\sigma+i\infty} A_1(s) e^{st} ds, \\ A_2(t) &= \frac{e^{-i\omega_{12}t}}{2\pi i} \int_{\sigma-i\infty}^{\sigma+i\infty} A_2(s - i\omega_{12}) e^{st} ds.\end{aligned}\quad (6)$$

Here the real constant  $\sigma$  is chosen so that  $s = \sigma$  lies to the right of all the singularities (poles and branch points) of  $A_i(s)$  ( $i = 1, 2$ ). Using the inverse Laplace transform, we obtain the expressions of the amplitudes (see Appendix B):

$$\begin{aligned}A_1(t) &= \sum_j \frac{f_1(x_j^{(1)})}{G'(x_j^{(1)})} e^{x_j^{(1)}t} + \sum_j \frac{f_1(x_j^{(2)})}{H'(x_j^{(2)})} e^{x_j^{(2)}t} \\ &\quad - \frac{e^{i\omega_{1c}t}}{\pi i} \int_0^\infty \frac{K_1(x)}{R_1(x) + R_2(x)} e^{-xt} dx,\end{aligned}\quad (7)$$

$$\begin{aligned}A_2(t) &= e^{-i\omega_{12}t} \left[ \sum_j \frac{f_2(x_j^{(1)})}{G'(x_j^{(1)})} e^{x_j^{(1)}t} + \sum_j \frac{f_2(x_j^{(2)})}{H'(x_j^{(2)})} e^{x_j^{(2)}t} \right] \\ &\quad - \frac{e^{i\omega_{2c}t}}{\pi i} \int_0^\infty \frac{K_2(x)}{R_1(x) + R_2(x)} e^{-xt} dx,\end{aligned}\quad (8)$$

where the functions are defined as

$$\begin{aligned}f_1(x) &= (x - i\omega_{12})[A_1(0)(x - i\omega_{12}) + A_2(0)x]/(2x - i\omega_{12}), \\ f_2(x) &= x[A_1(0)(x - i\omega_{12}) + A_2(0)x]/(2x - i\omega_{12}), \\ G(x) &= x(x - i\omega_{12}) - i\beta^{3/2}(2x - i\omega_{12})/(\sqrt{\omega_c} + \sqrt{-ix - \omega_{1c}}), \\ H(x) &= x(x - i\omega_{12}) - i\beta^{3/2}(2x - i\omega_{12})/(\sqrt{\omega_c} - i\sqrt{ix + \omega_{1c}}), \\ K_1(x) &= \beta^{3/2}\sqrt{-ix}(x - i\omega_{2c})(\omega_c - ix) \\ &\quad \times [A_1(0)(x - i\omega_{2c}) + A_2(0)(x - i\omega_{1c})], \\ K_2(x) &= \beta^{3/2}\sqrt{-ix}(x - i\omega_{1c})(\omega_c - ix) \\ &\quad \times [A_1(0)(x - i\omega_{2c}) + A_2(0)(x - i\omega_{1c})], \\ R_1(x) &= [(x - i\omega_{1c})(x - i\omega_{2c})(\omega_c - ix) \\ &\quad + i\beta^{3/2}(2x - i\omega_{1c} - i\omega_{2c})\sqrt{\omega_c}]^2, \\ R_2(x) &= ix\beta^3(2x - i\omega_{1c} - i\omega_{2c})^2,\end{aligned}$$

where  $x_j^{(1)}$  are the roots of the equation  $G(x) = 0$  in the region ( $\text{Im}(x_j^{(1)}) > \omega_{1c}$  or  $\text{Re}(x_j^{(1)}) > 0$ ), and  $x_j^{(2)}$  are the roots of the equation  $H(x) = 0$  in the region ( $\text{Im}(x_j^{(2)}) < \omega_{1c}$  and  $\text{Re}(x_j^{(2)}) < 0$ ). With the help of numerical calculation, we found that there are at least one root and at most two roots. We can classify these roots into two types:

- (i) pure imaginary root  $x_j^{(1)}$  with its imaginary part larger than  $\omega_{1c}$ ;
- (ii) complex root  $x_j^{(2)}$  with a negative real part and an imaginary part smaller than  $\omega_{1c}$ .

As for the pure imaginary roots, it is easy to prove analytically that there are two, one or no pure imaginary roots (see Appendix C). If

$$\omega_{1c} \leq \Delta_1 = \frac{\omega_{12}}{2} + \frac{\beta^{3/2}}{\sqrt{\omega_c}} - \sqrt{\left(\frac{\omega_{12}}{2}\right)^2 + \frac{\beta^3}{\omega_c}},$$

there are two pure imaginary roots  $ib_1, ib_2$  in the ranges  $\max(0, \omega_{1c}) < b_1 < \omega_{12}/2$ ,  $b_2 > \omega_{12}$ . If

$$\Delta_1 < \omega_{1c} \leq \Delta_2 = \frac{\omega_{12}}{2} + \frac{\beta^{3/2}}{\sqrt{\omega_c}} + \sqrt{\left(\frac{\omega_{12}}{2}\right)^2 + \frac{\beta^3}{\omega_c}},$$

there is only one pure imaginary root  $ib_2$ , which is in the range  $b_2 > \max(\omega_{1c}, \omega_{12})$ . If  $\omega_{1c} > \Delta_2$ , there are no pure imaginary roots. The number and the characteristics of the roots depend on the relative position of the two upper levels from the band edge. For example, we have five regions in the space of  $(\omega_{1c}, \omega_{12})$  with  $\omega_c = 100\beta$  (as shown in Fig. 2) according to the number and the values of the roots. There are two pure imaginary roots in region I, only one pure imaginary root in region II, one complex root and one pure imaginary root in region III, only one complex root in region IV, two complex roots in region V. It is obvious that the number and the characteristics of these roots in the present case are different from that in the isotropic dispersion relation case [8], such as the pure imaginary root always exists in the isotropic case. In the following discussion, we can see that these roots are directly related to the radiation field emitted by the atom and the population of two upper levels.

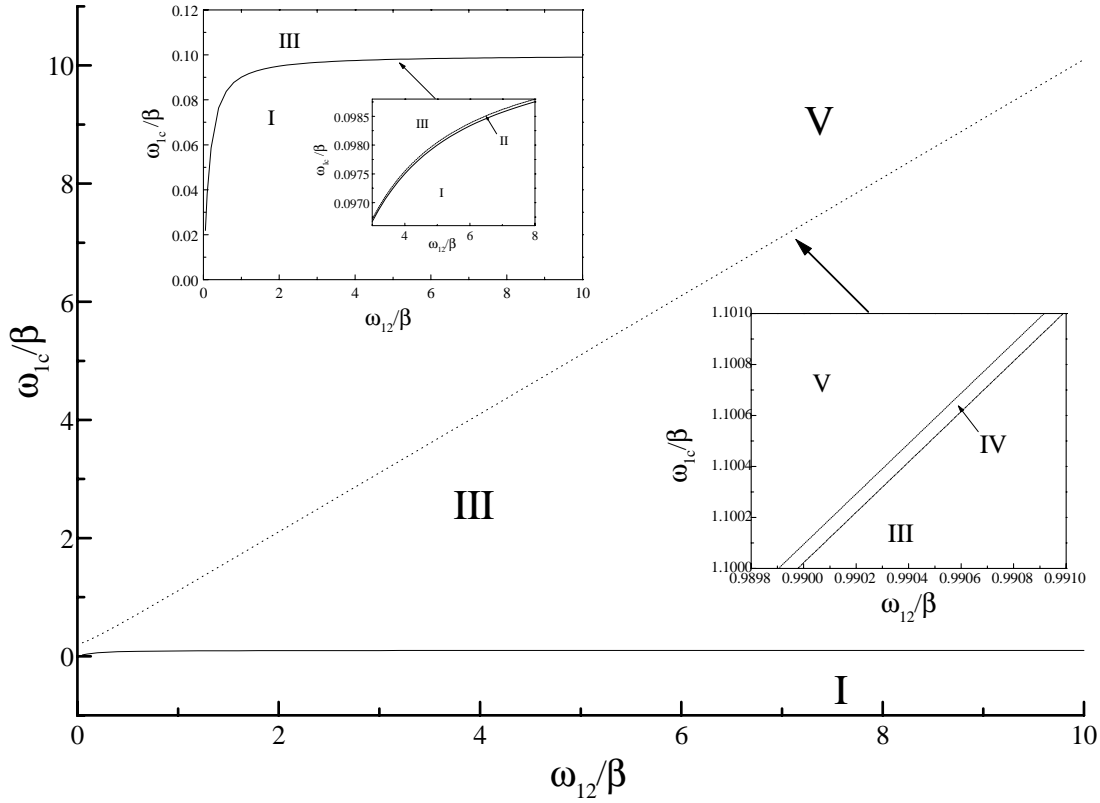


Fig. 2. The region for roots in the case:  $\omega_c = 100\beta$ .

### 3 The radiation field

The radiation field at a particular space point  $\mathbf{r}$ , can be written as [12]:

$$\mathbf{E}(\mathbf{r}, t) = \sum_k \sqrt{\frac{\hbar\omega_k}{2\epsilon_0 V}} e^{-i(\omega_k t - \mathbf{k}\cdot\mathbf{r})} B_k(t) \mathbf{e}_k \quad (9)$$

where

$$B_k(t) = g_k \int_0^t [A_1(t') e^{i(\omega_k - \omega_1)t'} + A_2(t') e^{i(\omega_k - \omega_2)t'}] dt'. \quad (10)$$

We can obtain the radiated field  $\mathbf{E}(\mathbf{r}, t)$  from  $A_1(t)$ ,  $A_2(t)$ . From equations (7, 8), we found  $\mathbf{E}(\mathbf{r}, t)$  can be expressed as the sum of three parts:  $\mathbf{E}_l(\mathbf{r}, t)$ ,  $\mathbf{E}_p(\mathbf{r}, t)$  and  $\mathbf{E}_d(\mathbf{r}, t)$

$$\mathbf{E}(\mathbf{r}, t) = \mathbf{E}_l(\mathbf{r}, t) + \mathbf{E}_p(\mathbf{r}, t) + \mathbf{E}_d(\mathbf{r}, t). \quad (11)$$

The first part  $\mathbf{E}_l(\mathbf{r}, t) = \sum_j \mathbf{E}_l^j(\mathbf{r}, t)$  comes from the first term in equations (7, 8).  $\mathbf{E}_l^j(\mathbf{r}, t)$  can be expressed as:

$$\mathbf{E}_l^j(\mathbf{r}, t) = \mathbf{E}_l^j(0) \frac{1}{r} e^{-i(\omega_1 - b_j^{(1)})t - r/l_j} \Theta\left[t - \frac{l_j r}{2A}\right], \quad (12)$$

where

$$\mathbf{E}_l^j(0) = \frac{\omega_1 d_1}{8A\pi\epsilon_0 i} \frac{f_3(x_j^{(1)})}{G'(x_j^{(1)})} \sum_n e^{i\mathbf{k}_0^n \cdot \mathbf{r}} \left[ \mathbf{u} - \frac{\mathbf{k}_0^n (\mathbf{k}_0^n \cdot \mathbf{u})}{(k_0^n)^2} \right]$$

with  $f_3(x) = A_1(0)(x - i\omega_{12}) + A_2(0)x$ , and  $x_j^{(1)} = ib_j^{(1)}$  is pure imaginary root.  $\Theta(x)$  is the Heaviside step function.

$$\Theta(x) = \begin{cases} 0 & x < 0, \\ 1 & x \geq 0. \end{cases}$$

The frequency of  $\mathbf{E}_l^j(\mathbf{r}, t)$  is  $(\omega_1 - b_j^{(1)})$ , which is smaller than  $\omega_c$  and within the forbidden band. Obviously,  $\mathbf{E}_l^j(\mathbf{r}, t)$  represents a localized mode in the localized field. The amplitude of the localized mode drops exponentially against the distance from the atom as  $e^{-r/l_j}$ . The size of the localized field is determined by the localization length,  $l_j = [(-ix_j^{(1)} - \omega_{1c})/A]^{-1/2}$ . The localized field  $\mathbf{E}_l(\mathbf{r}, t)$  does not decay against time and its distribution with its energy is trapped in the vicinity of the atom. The population in the lower level can jump back to the upper levels by absorbing the photon in the localized field, which forms dressed states leading to fractionalized steady-state atomic population in the excited state. If there are two localized modes in the localized field, the quantum interference between the two localized modes will lead to population oscillation in the two upper levels.

The second part  $\mathbf{E}_p(\mathbf{r}, t) = \sum_j \mathbf{E}_p^j(\mathbf{r}, t)$  comes from the second term in equations (7, 8). The expression of  $\mathbf{E}_p^j(\mathbf{r}, t)$  is:

$$\mathbf{E}_p^j(\mathbf{r}, t) = \mathbf{E}_p^j(0) \frac{1}{r} e^{(x_j^{(2)} - i\omega_1)t + iq_j r} \times \Theta\left(t - \frac{r}{2A(\text{Re} + \text{Im})(q_j)}\right), \quad (13)$$

where  $q_j = [(ix_j^{(2)} + \omega_{1c})/A]^{1/2}$ , and

$$\mathbf{E}_p^j(0) = \frac{\omega_1 d_1}{8A\pi\epsilon_0 i} \frac{f_3(x_j^{(2)})}{H'(x_j^{(2)})} \sum_n e^{ik_0^n \cdot \mathbf{r}} \left[ \mathbf{u} - \frac{\mathbf{k}_0^n (\mathbf{k}_0^n \cdot \mathbf{u})}{(k_0^n)^2} \right].$$

$x_j^{(2)} = a_j^{(2)} + ib_j^{(2)}$  with  $a_j^{(2)} < 0$  and  $b_j^{(2)} < \omega_{1c}$  is a complex root. The frequency of  $\mathbf{E}_p^j(r, t)$  is  $(\omega_1 - b_j^{(2)})$ , which is larger than  $\omega_c$ , and within the transmitting band.  $\mathbf{E}_p^j(r, t)$  is a propagating mode in the radiation field emitted by the atom. With the fact that the phase difference between any two points in space is fixed,  $\mathbf{E}_p^j(r, t)$  travels away coherently from the atom in the form of an exponential pulse with the phase velocity

$$v_p = \sqrt{A}(\omega_1 - b_j^{(2)})/\text{Re}(\sqrt{\omega_{1c} + ix_j^{(2)}})$$

and the energy velocity

$$v_e = \sqrt{A}a_j^{(2)}/\text{Im}(\sqrt{\omega_{1c} + ix_j^{(2)}}).$$

The third part  $\mathbf{E}_d(r, t)$  comes from the integration along the cut of the single valued branches in equations (7, 8)

$$\begin{aligned} \mathbf{E}_d(r, t) = \mathbf{E}_d(0) \frac{1}{r} e^{-i\omega_c t + \frac{ix^2}{4At} + \frac{3i\pi}{4}} \int_0^\infty \frac{K_1(x) + K_2(x)}{R_1(x) + R_2(x)} dx \\ \times \int_{-\infty}^\infty \frac{[ye^{3\pi i/4} + r/(2\sqrt{At})]e^{-y^2} dy}{-xt + i[ye^{3\pi i/4} + r/(2\sqrt{At})]^2}, \end{aligned} \quad (14)$$

where

$$\mathbf{E}_d(0) = \frac{\omega_1 d_1}{8A\pi^3 \epsilon_0} \sum_n e^{ik_0^n \cdot \mathbf{r}} \left[ \mathbf{u} - \frac{\mathbf{k}_0^n (\mathbf{k}_0^n \cdot \mathbf{u})}{(k_0^n)^2} \right].$$

The evolution of  $\mathbf{E}_d(\mathbf{r}, t)$  from the atom as a function of the time  $t$  and the distance  $r$  is given in Figure 3. As time  $t$  increases,  $\mathbf{E}_d(\mathbf{r}, t)$  at any space point increases firstly from zero to a maximum value, and then after that decreases to zero again. As the distance  $r$  from the atom increases,  $\mathbf{E}_d(\mathbf{r}, t)$  also has the similar behavior at a fixed time. The position of the maximum  $\mathbf{E}_d(\mathbf{r}, t)$  goes away from the atom with time. In long time limit, we have approximately

$$\mathbf{E}_d(r, t) \sim t^{-3/2} e^{-i\omega_c t + ir^2/(4At)}.$$

From the above expression, we can see that this field behaves as a power law decay and there is no fixed phase difference between any two space points. The energy diffuses out incoherently, and this field represents a typical diffusion field. Moreover, we can find that the localized  $\mathbf{E}_l(\mathbf{r}, t)$  and propagating field  $\mathbf{E}_p(\mathbf{r}, t)$  behave with the well-defined frequencies  $\omega_1 - b^{(1,2)}$ . But for the diffusion field, we could not find a well-defined frequency, although its energy propagates out.

The radiation field emitted by the atom is characterized by the three different fields, the localized field, the propagating field and the diffusion field. Their amplitudes depend strongly on the relative position between the two

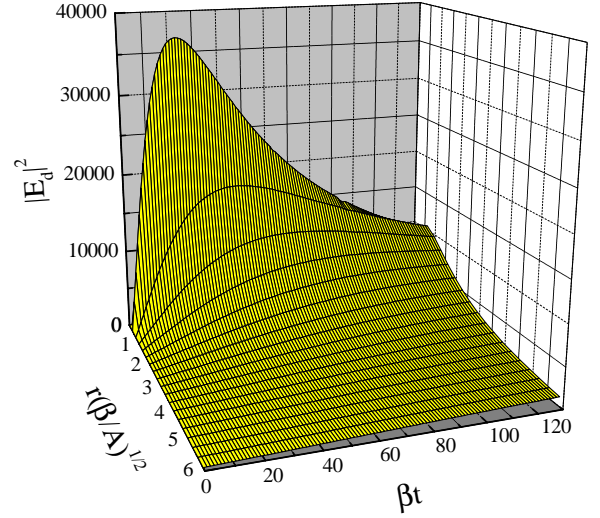


**Fig. 3.** The diffusion field (in arbitrary unit) as a function of the scaled time  $\beta t$  and distance  $r(\beta/A)^{1/2}$ . Here  $\omega_c = 200\beta$ ,  $\omega_{12} = 8.6\beta$ ,  $\omega_{1c} = 0.070131\beta$ .

upper levels and the band edge. For the localized field, the amplitude of the localized mode  $\mathbf{E}_l^j(\mathbf{r}, t)$  decreases (as shown in Fig. 4), and its localized length increases as the relative position  $\omega_{1c}$  increases. When  $\omega_{1c}$  tends to  $\Delta_1$  (or  $\Delta_2$ ), the amplitude of  $\mathbf{E}_l^1(\mathbf{r}, t)$  (or  $\mathbf{E}_l^2(\mathbf{r}, t)$ ) tends to zero, and its localized length tends to infinity. For the propagating field, the amplitude of the propagating mode  $\mathbf{E}_p^j(\mathbf{r}, t)$  also decreases as  $\omega_{1c}$  increases (see Fig. 4). When the relative position  $\omega_{1c}$  changes from region II to region III (or from region IV to region V), there is a pronounced switch-on effect for the propagating mode  $\mathbf{E}_p^1(\mathbf{r}, t)$  (or the propagating mode  $\mathbf{E}_p^2(\mathbf{r}, t)$ ). These sudden increases of the propagating modes can be used to design an active optical multi-channel micro-sized switch. Furthermore, the amplitude of the diffusion field changes with the variation of the relative position  $\omega_{1c}$  and there are two regions where the diffusion field is extremely strong (as shown in Fig. 5). Comparing Figures 2 and 5, we find that the position and width of the two regions with regard to the relative position  $\omega_{1c}$  is just corresponding to regions II and IV in Figure 2. In above section, we have narrated that the width of region II corresponds to the existence range of only one pure imaginary root and the width of region IV is the existence range of only one complex root. We can obtain the width of the two regions in regard to  $\omega_{1c}$  for a given  $\omega_{12}$  through numerical calculation. So the width of the diffusion field is also obtained. We note that the diffusion field in region II (or region IV) is almost several hundred times stronger than that in regions I, III and V. The diffusion fields in regions I, III and V are extremely small and can be neglected.

Therefore, there is direct relation between the properties of the radiation field and the relative position of the two upper levels from the band edge. The main components of the emitted radiation are two localized modes  $\mathbf{E}_l^1(\mathbf{r}, t)$  and  $\mathbf{E}_l^2(\mathbf{r}, t)$  in region I, one localized mode  $\mathbf{E}_l^2(\mathbf{r}, t)$  and a strong diffusion field in region II, one

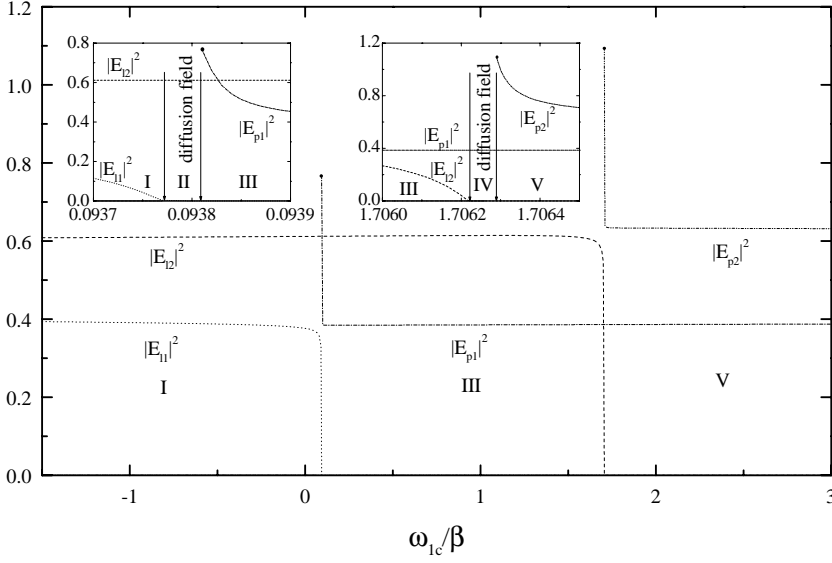


**Fig. 4.** The amplitude square (in arbitrary unit) of the localized modes and the propagating modes as functions of the relative position  $\omega_{1c}$  with  $\omega_c = 100\beta$ ,  $\omega_{12} = 1.6\beta$ ,  $r\sqrt{\beta/A} = 1$ ,  $\beta t = 3$ , and  $|\Phi(0)\rangle = (|a_1\rangle + |a_2\rangle)/\sqrt{2}$ .

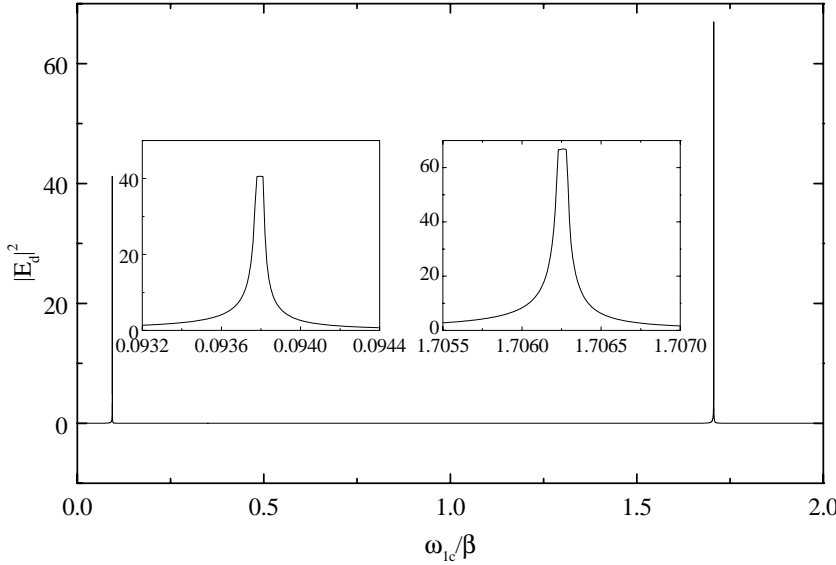


**Fig. 5.** The amplitude square (in arbitrary unit) of the diffusion field as a function of the transition frequency  $\omega_{1c}$  with  $\omega_c = 100\beta$ ,  $\omega_{12} = 1.6\beta$ ,  $r\sqrt{\beta/A} = 1$  and  $\beta t = 3$  and  $|\Phi(0)\rangle = (|a_1\rangle + |a_2\rangle)/\sqrt{2}$ .

localized mode  $\mathbf{E}_l^2(\mathbf{r}, t)$  and one propagating mode  $\mathbf{E}_p^1(\mathbf{r}, t)$  in region III, one propagating mode  $\mathbf{E}_p^1(\mathbf{r}, t)$  and a strong diffusion field in region IV, two propagating modes  $\mathbf{E}_p^1(\mathbf{r}, t)$  and  $\mathbf{E}_p^2(\mathbf{r}, t)$  in region V.

Considering the process of the upper levels move from in the forbidden gap to deep in the transmitting band, we can get the following picture of the energy translation among the three different fields. When the relative position  $\omega_{1c}$  increases to  $\Delta_1$ , the frequency of the localized mode  $\mathbf{E}_l^1(\mathbf{r}, t)$  is  $\omega_c$ , and the amplitude of  $\mathbf{E}_l^1(\mathbf{r}, t)$  decreases to zero. From Figures 4 and 5, we can see that the energy corresponding to  $\mathbf{E}_l^1(\mathbf{r}, t)$  has been transferred to the diffusion field. In region II, the change of the energy of the localized field with the localized mode  $\mathbf{E}_l^2(\mathbf{r}, t)$  and the diffusion field is not obvious. As  $\omega_{1c}$  changes from region II to region III, the propagating field with the propagating mode  $\mathbf{E}_p^1(\mathbf{r}, t)$  begins to appear and the energy of the diffusion field is transferred to it. Similarly, when  $\omega_{1c}$  increases

to  $\Delta_2$ , the frequency of the localized mode  $\mathbf{E}_l^2(\mathbf{r}, t)$  is  $\omega_c$ , and the amplitude of  $\mathbf{E}_l^2(\mathbf{r}, t)$  decreases to zero. The energy of the localized field with the localized mode  $\mathbf{E}_l^2(\mathbf{r}, t)$  has been transferred to the diffusion field. In region IV, the energy of the propagating field with the propagating mode  $\mathbf{E}_p^1(\mathbf{r}, t)$  and the diffusion field is changeless. When  $\omega_{1c}$  goes from region IV to region V, the amplitude of the diffusion field decreases and the energy of the diffusion field is transferred to the propagating field with the propagating mode  $\mathbf{E}_p^2(\mathbf{r}, t)$ .

The radiation properties in the present system are different from that in the case with the isotropic dispersion relation. The diffusion field also exists in isotropic case, but it is so small that it is negligible all over the photonic crystal [8]. For the anisotropic model, there are two regions II and IV where the diffusion field becomes important and can not be ignored. In the anisotropic dispersion case, the localized field can disappear in region IV and V in Figure 2. In the isotropic dispersion model, such

regions do not exist, and the localized field always exists. Such different properties of the emitted field result from the difference of DOS near the band edge in the two cases. The DOS in the isotropic case leads to a singularity at the band edge, which does not exist in the anisotropic case. In the isotropic case, the frequency of the localized field cannot be the frequency of the band edge  $\omega_c$  because of the infinite DOS at  $\omega_c$ . An infinite DOS means infinite energy requirement for the localized field. This is why we always have the localized field and such regions IV and V do not exist in the isotropic case. In the anisotropic case, the frequency can be  $\omega_c$  because the DOS is zero at  $\omega_c$ , and when it is  $\omega_c$ , the localized field disappears (frequency larger than  $\omega_c$  is in the band).

#### 4 The population in the two upper levels

In this section we discuss mainly the influence of the anisotropic dispersion relation on the population in the two upper levels.

From the previous work [4–10], we know that for a three-level atom with transition frequencies close to the band edge in the isotropic crystal, the localized field, the propagating field and the diffusion field can dress the atom simultaneously, which leads to splitting of the upper levels into “dressed states” or “quasi-dressed states”. Strong quantum interference between the “dressed states” or “quasi-dressed states” leads to oscillatory or quasioscillatory behavior of the upper levels population, which is quite distinct from the exponential decay in an ordinary vacuum. A fractionalized steady-state population is trapped in the upper level forever because of the always existence of a localized field, even when the resonant transition frequencies lie deep inside the transmitting band.

In present anisotropic case, the population in the two upper levels of the atom can be obtained from equations (7, 8),  $P_1(t) = |A_1(t)|^2$ ,  $P_2(t) = |A_2(t)|^2$ , and the total population is  $P(t) = P_1(t) + P_2(t)$ . The first term in equations (7, 8) comes from pure imaginary roots corresponding to the localized field which results in the photon-atom bound dressed states without decay. While the second term in equations (7, 8) comes from complex roots corresponding to the propagating field which results in the photon-atom bound dressed states decaying in time. The integration along the cut of the single valued branch in equations (7, 8) corresponding to the diffusion field yield the quasi-dressed state decaying in time, too. The quantum interference between the dressed states or the dressed state and quasi-dressed state leads to oscillatory (Fig. 6) or quasi-oscillatory (Figs. 7, 8, 10, 11) behavior of spontaneous emission decay.

From the discussion in above section, we know that the properties of the radiation field change with the variation of the relative position of the two upper levels from the band edge, and the properties of the radiation field are different from each other in the regions in Figure 2. Here the population in the two upper levels depends not only on the relative position of the two upper levels from the band edge but also the initial atomic states. In the

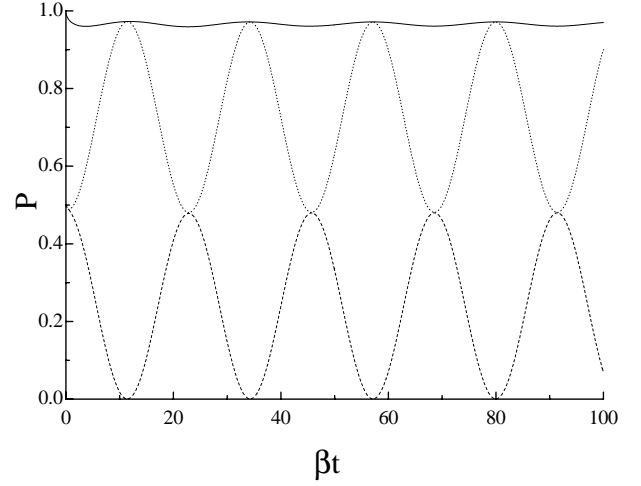


**Fig. 6.** Atomic population on the upper levels  $P_1(t)$  (dashed curve),  $P_2(t)$  (dotted curve) and  $P(t)$  (solid curve) as a function of the scaled time  $\beta t$ . Here  $\omega_c = 100\beta$ ,  $\omega_{12} = 0.2\beta$ ,  $\omega_{1c} = 0.0178\beta$ ,  $|\Phi(0)\rangle = (|a_1\rangle + |a_2\rangle)/\sqrt{2}$ .

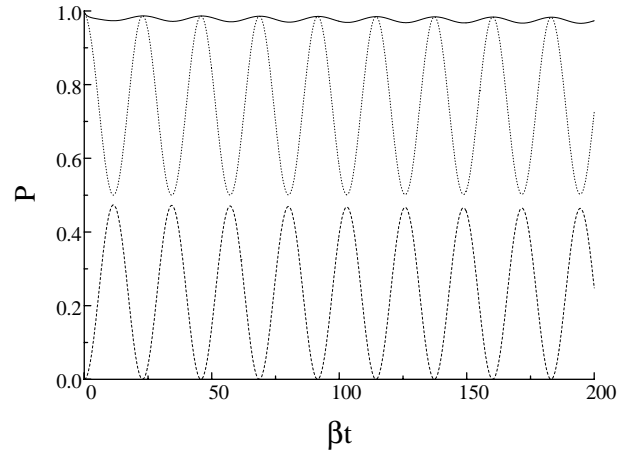


**Fig. 7.** Atomic population on the upper levels  $P_1(t)$  (dashed curve),  $P_2(t)$  (dotted curve) and  $P(t)$  (solid curve) as a function of the scaled time  $\beta t$ . Here  $\omega_c = 100\beta$ ,  $\omega_{12} = 0.2\beta$ ,  $\omega_{1c} = 0.058581\beta$ ,  $|\Phi(0)\rangle = |a_2\rangle/\sqrt{2}$ .

following, we investigate the properties of the population in the two upper levels when the upper levels move from in the forbidden gap to deep in the transmitting band corresponding to the five regions in Figure 2.

In region I in Figure 2, the relative position  $\omega_{1c} < \Delta_1$ , and the emission in this region is a localized field with two localized modes which dress the atom to form two dressed states without decay. The quantum interference between the two dressed states leads to oscillatory periodic behavior of the population for large time  $t$  (see Fig. 6). The oscillatory behavior of the population represents the transfer of population from  $|a_1\rangle$  to  $|a_2\rangle$  or *vice versa* and indicates that the transfer of population between the two upper levels always exists. Moreover, there will be more population transferring between the two upper levels if the two upper levels get so close that the transfer of population becomes easily. The period of the oscillations for  $P_1(t)$ ,  $P_2(t)$

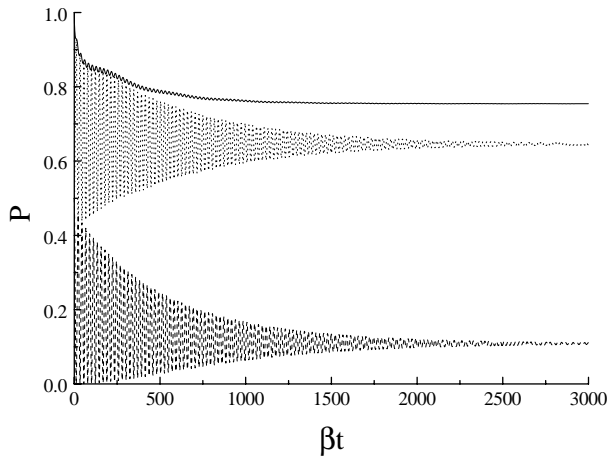


**Fig. 8.** Atomic population on the upper levels  $P_1(t)$  (dashed curve),  $P_2(t)$  (dotted curve) and  $P(t)$  (solid curve) as a function of the scaled time  $\beta t$ . Here  $\omega_c = 100\beta$ ,  $\omega_{12} = 0.2\beta$ ,  $\omega_{1c} = 0.321405\beta$ ,  $|\Phi(0)\rangle = (|a_1\rangle + |a_2\rangle)/\sqrt{2}$ .

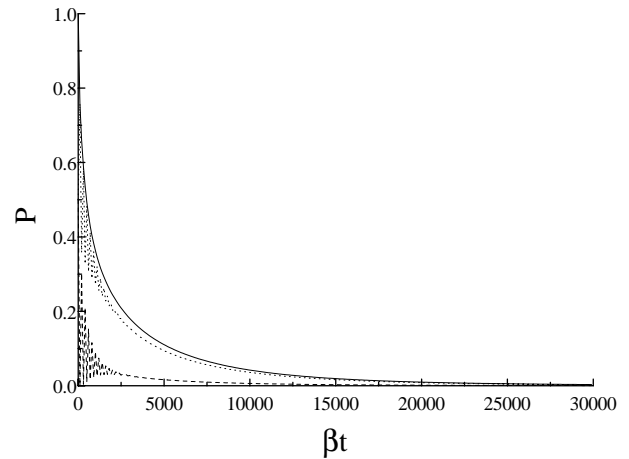


**Fig. 10.** Atomic population on the upper levels  $P_1(t)$  (dashed curve),  $P_2(t)$  (dotted curve) and  $P(t)$  (solid curve) as a function of the scaled time  $\beta t$ . Here  $\omega_c = 100\beta$ ,  $\omega_{12} = 0.2\beta$ ,  $\omega_{1c} = 0.341555\beta$ ,  $|\Phi(0)\rangle = (|a_1\rangle + |a_2\rangle)/\sqrt{2}$ .

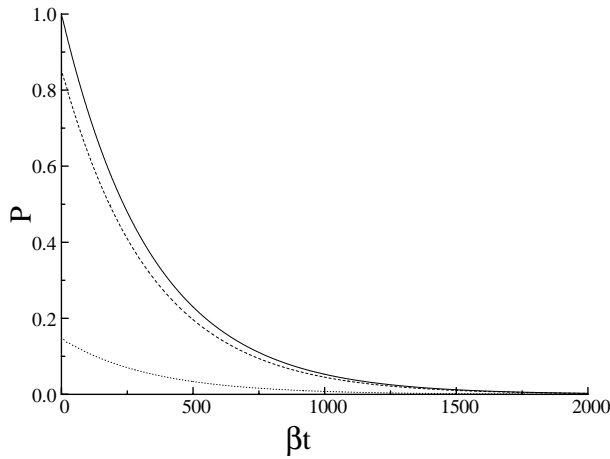


**Fig. 9.** Atomic population on the upper levels  $P_1(t)$  (dashed curve),  $P_2(t)$  (dotted curve) and  $P(t)$  (solid curve) as a function of the scaled time  $\beta t$ . Here  $\omega_c = 100\beta$ ,  $\omega_{12} = 0.2\beta$ ,  $\omega_{1c} = 0.31068\beta$ ,  $|\Phi(0)\rangle = 0.925457525|a_1\rangle - 0.378851517|a_2\rangle$ .

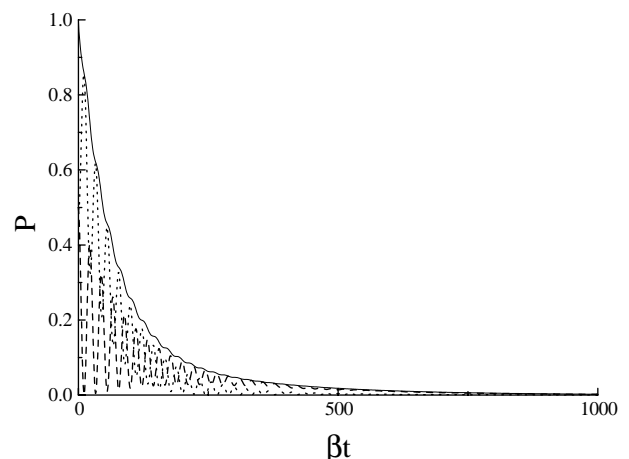


**Fig. 11.** Atomic population on the upper levels  $P_1(t)$  (dashed curve),  $P_2(t)$  (dotted curve) and  $P(t)$  (solid curve) as a function of the scaled time  $\beta t$ . Here  $\omega_c = 100\beta$ ,  $\omega_{12} = 0.2\beta$ ,  $\omega_{1c} = 0.58036\beta$ ,  $|\Phi(0)\rangle = (|a_1\rangle + |a_2\rangle)/\sqrt{2}$ .

is  $2\pi/(b_1^{(1)} - b_2^{(1)})$  ( $ib_1^{(1)}$  and  $ib_2^{(1)}$  are two pure imaginary roots). Although the oscillation amplitudes  $K_1$  of  $P_1(\infty)$  and  $K_2$  of  $P_2(\infty)$  depend on the initial state, the ratio of the amplitudes is independent of the initial state, which is

$$\frac{K_1}{K_2} = \frac{(b_1^{(1)} - \omega_{12})(\omega_{12} - b_2^{(1)})}{b_1^{(1)}b_2^{(1)}}.$$

The phase difference of the two periodic oscillations is  $\pi$ , and the phase angle of the total population  $P(t)$  in the excited states is the same as that of the population  $P_2(t)$  in the upper level  $|a_2\rangle$ .

There are a localized field and a diffusion field when  $\omega_{1c}$  within region II. The localized field dresses the atom to form a non-decaying dressed state. In this region, the diffusion field is so strong that it can not be ignored and makes the atom dressed to form a quasi-dressed state decaying in time. In the region III, the main components

of the emitted radiation are one localized mode and one propagating mode. The dressed state resulting from the propagating mode also decay in time. The quantum interference between the dressed states or the dressed state and the quasi-dressed state leads to the quasi-oscillatory behavior of the population (see Figs. 7 and 8). Comparing Figures 7 and 8, we notice that the decay of the population in Figure 7 is more slow than that in Figure 8. The reason is that the diffusion field causes the upper-level population decay in a manner of the power law while the propagating field makes the upper-level population decay exponentially. These decays are more slow than that in the case of the isotropic dispersion relation and the population oscillate many cycles ( $\sim 10^3$ ) before eventually decay to their final values. This is because that the energy can travel away from the atom along all the directions in the isotropic case, while the energy can travel away from the atom along some directions in the anisotropic case. When time goes to



infinity, there is only the dressed state without decay having contribution to the population, and  $P(t), P_1(t), P_2(t)$  tend to constants  $P_0, P_{10}, P_{20}$  resulting in a fractionalized steady-state population trapped in the upper levels forever. The amount of population trapped in the upper levels depends on the initial condition. As  $t \rightarrow \infty$ ,  $P_{10}, P_{20}$  are directly proportional to  $|A_1(0)(b_1^{(1)} - \omega_{12}) + A_2(0)b_1^{(1)}|^2$  ( $ib_1^{(1)}$  is the pure imaginary root). We can prove that  $P_{10}, P_{20}$  can be minimized  $P_{10} = 0, P_{20} = 0$  by choosing the initial state  $A_1(0)/A_2(0) = -b_1^{(1)}/(b_1^{(1)} - \omega_{12})$  (see Fig. 9). There is no population in the upper levels and this means the complete decay of population.

As it has been mentioned in the above sections, the localized field does not exist in region IV and V in Figure 2. The emission radiation contains only one propagating mode in region IV or two propagating mode in region V. The propagating field dresses the atom to form a decaying dressed state. Similar to region II, the diffusion field in region IV is also so strong that it can not be ignored and makes the atom dressed to form a quasi-dressed state decaying in time. The quantum interference between the dressed state and the quasi-dressed state in region IV (see Fig. 10) or the quantum interference between the two dressed states in region V (see Fig. 11) can both lead to the quasi-oscillatory behavior of the population. In the same way, comparing Figures 10 and 11, we can see that the decay of the population in Figure 10 is more slow than that in Figure 11. There is no localized field and the energy in propagating field or diffusion field can traveling away from the atom. So the amount of the population can decay to zero as time goes to infinity and realize the complete decay of population for any initial state (see Figs. 10 and 11). This complete decay of population does not depend on the initial state which is different from that in the case of the isotropic dispersion relation. While in the case of the isotropic dispersion relation, the localized field always exists no matter what the relative position of the two upper levels from the band edge are. So there is no complete decay of population unless by choosing specific initial state.

## 5 Conclusions

In summary, we have derived some interesting features of spontaneous emission from a three-level atom embedded in photonic crystals in which the anisotropic dispersion relation is taken into account. Because of no singularity in DOS, these features are different from that in the isotropic case. Besides the localized field and propagating field, there is a distinct diffusion field in some regions. The localized field can disappear which is due to no existence of singularity in DOS. The population displays oscillatory, quasi-oscillatory or complete decay behavior, depending on the initial state and the relative position of the upper levels from the band edge. The complete decay can also be realized with any initial state in certain condition.

This work was supported in part by the Shanghai Educational Council and FRG from Hong Kong Baptist University.

## Appendix A: The calculation of $\Gamma$

The coupling constants  $g_k^{(j)}$  ( $j = 1, 2$ ) may be written in the form

$$g^{(j)} = \frac{\omega_j d_j}{\hbar} \left( \frac{\hbar}{2\epsilon_0 \omega_k V} \right)^{1/2} \mathbf{e}_k \cdot \mathbf{u}_j, \quad (\text{A.1})$$

where  $\mathbf{u}_j$  are the unit vectors of the atomic dipole moments,  $\mathbf{e}_k$  are the two transverse unit vectors.

We first calculate  $\Gamma_{11}$ ,

$$\begin{aligned} \Gamma_{11} &= \sum_k \frac{g_k^{(1)} g_k^{(1)}}{s - i(\omega_1 - \omega_k)} \\ &= \frac{(\omega_1 d_1)^2}{2\epsilon_0 \hbar V} \sum_k \frac{(\mathbf{e}_k \cdot \mathbf{u}_1)(\mathbf{e}_k \cdot \mathbf{u}_1)}{\omega_k [s - i(\omega_1 - \omega_k)]} \\ &= \frac{(\omega_1 d_1)^2}{16\epsilon_0 \hbar \pi^3} \iiint \frac{d^3 \mathbf{k}}{\omega_k [s - i(\omega_1 - \omega_k)]} \\ &\quad \times \left[ 1 - \frac{(\mathbf{k} \cdot \mathbf{u}_1)(\mathbf{k} \cdot \mathbf{u}_1)}{k^2} \right]. \end{aligned} \quad (\text{A.2})$$

Here we have replaced the sum by an integral *via*

$$\sum_k \rightarrow \frac{V}{(2\pi)^3} \iiint d^3 \mathbf{k}$$

and used  $\mathbf{q} = \mathbf{k} - \mathbf{k}_0^n$ . There are eight symmetry points  $\mathbf{k}_0^n$  ( $n = 1, 2, \dots, 8$ ) in the diamond dielectric structure and the dispersion relation  $\omega_k = \omega_c + A|\mathbf{k} - \mathbf{k}_0^n|^2$  can be turned into the form  $\omega_k = \omega_c + A|\mathbf{k} - \mathbf{k}_0^n|^2$  for this structure. Assuming  $\mathbf{k} = (k \sin \theta \cos \phi, k \sin \theta \sin \phi, k \cos \theta)$ ,  $\mathbf{u}_1 = (0, 0, 1)$ . The angle  $\theta$  between the arbitrary  $\mathbf{k}$ , whose direction is near one of  $\mathbf{k}_0^n$ , and  $\mathbf{u}_1$  can be replaced by the angle  $\theta_n$  between  $\mathbf{k}_0^n$  and  $\mathbf{u}_1$  approximately. So we have

$$1 - \frac{(\mathbf{k} \cdot \mathbf{u}_1)(\mathbf{k} \cdot \mathbf{u}_1)}{k^2} = \sin^2 \theta_n.$$

Using the dispersion characteristics  $\omega_k = \omega_c + A|\mathbf{k} - \mathbf{k}_0^n|^2$ , we can get

$$\begin{aligned} \Gamma_{11} &= \frac{(\omega_1 d_1)^2}{16\epsilon_0 \hbar \pi^3} \left( \sum_{n=1}^8 \sin^2 \theta_n \right) \\ &\quad \times \iiint \frac{d^3 \mathbf{k}}{[\omega_c + A|\mathbf{k} - \mathbf{k}_0^n|^2][s + i(\omega_c - \omega_1) + iA|\mathbf{k} - \mathbf{k}_0^n|^2]} \\ &= \frac{(\omega_1 d_1)^2}{16\epsilon_0 \hbar \pi^3} \left( \sum_{n=1}^8 \sin^2 \theta_n \right) \iiint \frac{d^3 \mathbf{q}}{(\omega_c + Aq^2)(s - i\omega_{1c} + iAq^2)} \\ &= \frac{(\omega_1 d_1)^2}{4\epsilon_0 \hbar \pi^2} \left( \sum_{n=1}^8 \sin^2 \theta_n \right) \int_0^\infty \frac{q^2 dq}{(\omega_c + Aq^2)(s - i\omega_{1c} + iAq^2)} \\ &= -\frac{i\beta_1^{3/2}}{\sqrt{\omega_c + \sqrt{-\omega_{1c} - is}}} \end{aligned} \quad (\text{A.3})$$

where

$$\beta_1^{3/2} = \frac{(\omega_1 d_1)^2}{8\pi\epsilon_0 \hbar A^{3/2}} \left( \sum_{n=1}^8 \sin^2 \theta_n \right).$$

$$\begin{aligned}
\frac{1}{2\pi i} \int_{-\infty-i-0}^{\omega_{1c}i-0} \frac{f_1(x)}{G(x)} e^{xt} dx &= \sum_j \frac{f_1(x_j^{(1)})}{G'(x_j^{(1)})} e^{x_j^{(1)}t} - \frac{1}{2\pi i} \int_{\omega_{1c}i}^{-\infty+\omega_{1c}i} \frac{A_1(0)(x-i\omega_{12}) - \frac{[A_1(0)-A_2(0)]i\beta^{3/2}}{\sqrt{\omega_c+i\sqrt{-ix+\omega_{1c}}}}}{x(x-i\omega_{12}) - \frac{(2x-i\omega_{12})i\beta^{3/2}}{\sqrt{\omega_c+i\sqrt{-ix+\omega_{1c}}}}} e^{xt} dx \\
&= \sum_j \frac{f_1(x_j^{(1)})}{G'(x_j^{(1)})} e^{x_j^{(1)}t} + \frac{e^{i\omega_{1c}t}}{2\pi i} \int_0^\infty \frac{A_1(0)(i\omega_{2c}-x)(\omega_c-ix) - i\beta^{3/2}[A_1(0)-A_2(0)](\sqrt{\omega_c}-i\sqrt{-ix})}{(x-i\omega_{1c})(x-i\omega_{2c})(\omega_c-ix) + i\beta^{3/2}(2x-i\omega_{1c}-\omega_{2c})(\sqrt{\omega_c}-i\sqrt{-ix})} e^{-xt} dx \quad (B.2)
\end{aligned}$$

The phase angle is defined as  $-\frac{\pi}{2} < \arg \sqrt{-\omega_{1c} - is} < \frac{\pi}{2}$ .  
In the same way,  $\Gamma_{22}$  can be worked out

$$\Gamma_{22} = -\frac{i\beta_2^{3/2}}{\sqrt{\omega_c} + \sqrt{-\omega_{1c} - is}} \quad (A.4)$$

where

$$\beta_2^{3/2} = \frac{(\omega_2 d_2)^2}{8\pi\epsilon_0 \hbar A^{3/2}} \left( \sum_{n=1}^8 \sin^2 \theta_n \right).$$

When the two dipole moments of the two transitions are parallel to each other, *i.e.*,  $\mathbf{u}_1 = \mathbf{u}_2$ ,

$$\begin{aligned}
\Gamma_{12} &= \sum_k \frac{g_k^{(1)} g_k^{(2)}}{s - i(\omega_1 - \omega_k)} \\
&= \frac{\omega_1 d_1 \omega_2 d_2}{2\epsilon_0 \hbar V} \sum_k \frac{(\mathbf{e}_k \cdot \mathbf{u}_1)(\mathbf{e}_k \cdot \mathbf{u}_2)}{\omega_k [s - i(\omega_1 - \omega_k)]} \\
&= -\frac{i(\beta_1 \beta_2)^{3/4}}{\sqrt{\omega_c} + \sqrt{-\omega_{1c} - is}}. \quad (A.5)
\end{aligned}$$

Hence,  $\Gamma_{lm}$  can be written as follows:

$$\begin{aligned}
\Gamma_{11} &= -\frac{i\beta_1^{3/2}}{\sqrt{\omega_c} + \sqrt{-\omega_{1c} - is}}, \\
\Gamma_{22} &= -\frac{i\beta_2^{3/2}}{\sqrt{\omega_c} + \sqrt{-\omega_{1c} - is}}, \\
\Gamma_{12} &= -\frac{i(\beta_1 \beta_2)^{3/4}}{\sqrt{\omega_c} + \sqrt{-\omega_{1c} - is}} \quad (\text{parallel}).
\end{aligned}$$

## Appendix B: The calculation of $\mathbf{A}_1(\mathbf{t})$ , $\mathbf{A}_2(\mathbf{t})$ and $\mathbf{B}_k(\mathbf{t})$

Some functions are defined as follows:

$$f_1(x) = (x - i\omega_{12}) \frac{[A_1(0)(x - i\omega_{12}) + A_2(0)x]}{(2x - i\omega_{12})},$$

$$f_2(x) = x \frac{[A_1(0)(x - i\omega_{12}) + A_2(0)x]}{(2x - i\omega_{12})},$$

$$f_3(x) = A_1(0)(x - i\omega_{12}) + A_2(0)x,$$

$$G(x) = x(x - i\omega_{12}) - i\beta^{3/2} \frac{(2x - i\omega_{12})}{(\sqrt{\omega_c} + \sqrt{-ix - \omega_{1c}})},$$

$$H(x) = x(x - i\omega_{12}) - i\beta^{3/2} \frac{(2x - i\omega_{12})}{(\sqrt{\omega_c} - i\sqrt{-ix + \omega_{1c}})},$$

$$K_1(x) = \beta^{3/2} \sqrt{-ix}(x - i\omega_{2c})(\omega_c - ix) \times [A_1(0)(x - i\omega_{2c}) + A_2(0)(x - i\omega_{1c})],$$

$$K_2(x) = \beta^{3/2} \sqrt{-ix}(x - i\omega_{1c})(\omega_c - ix) \times [A_1(0)(x - i\omega_{2c}) + A_2(0)(x - i\omega_{1c})],$$

$$R_1(x) = [(x - i\omega_{1c})(x - i\omega_{2c})(\omega_c - ix) + i\beta^{3/2}(2x - i\omega_{1c} - i\omega_{2c})\sqrt{\omega_c}]^2,$$

$$R_2(x) = ix\beta^3(2x - i\omega_{1c} - i\omega_{2c})^2.$$

From  $G(x)$ ,  $H(x)$ , we can get

$$\begin{aligned}
G'(x) &= 2x - i\omega_{12} - \frac{2i\beta^{3/2}}{\sqrt{\omega_c} + \sqrt{-ix - \omega_{1c}}} \\
&\quad + \frac{(2x - i\omega_{12})\beta^{3/2}}{2\sqrt{-\omega_{1c} - ix}(\sqrt{\omega_c} + \sqrt{-ix - \omega_{1c}})^2}, \\
H'(x) &= 2x - i\omega_{12} - \frac{2i\beta^{3/2}}{\sqrt{\omega_c} - i\sqrt{-ix + \omega_{1c}}} \\
&\quad + \frac{(2ix + \omega_{12})\beta^{3/2}}{2\sqrt{\omega_{1c} + ix}(\sqrt{\omega_c} - i\sqrt{-ix + \omega_{1c}})^2}.
\end{aligned}$$

Using the inverse Laplace transform, we have

$$\begin{aligned}
A_1(t) &= \frac{1}{2\pi i} \int_{\sigma-i\infty}^{\sigma+i\infty} A_1(s) e^{st} ds = \frac{1}{2\pi i} \int_{\sigma-i\infty}^{\sigma+i\infty} \frac{f_1(x)}{G(x)} e^{xt} dx \\
&= \sum_j \frac{f_1(x_j^{(1)})}{G'(x_j^{(1)})} e^{x_j^{(1)}t} - \frac{1}{2\pi i} \left[ \int_{-\infty-i-0}^{\omega_{1c}i-0} + \int_{\omega_{1c}i+0}^{-\infty+i+0} \right] \\
&\quad \times \frac{f_1(x)}{G(x)} e^{xt} dx, \quad (B.1)
\end{aligned}$$

where  $x_j^{(1)}$  are the roots of the equation  $G(x) = 0$ , the real number  $\sigma$  is chosen so that  $x = \sigma$  lies to the right of all the singularities  $x_j^{(1)}$

*see equation (B.2) above.*

$$\begin{aligned} \frac{1}{2\pi i} \int_{\omega_{1c}i+0}^{-\infty i+0} \frac{f_1(x)}{G(x)} e^{xt} dx &= \frac{1}{2\pi i} \int_{\omega_{1c}i}^{-\infty i} \frac{f_1(x)}{H(x)} e^{xt} dx \\ &= - \sum_j \frac{f_1(x_j^{(2)})}{H'(x_j^{(2)})} e^{x_j^{(2)}t} - \frac{e^{i\omega_{1c}t}}{2\pi i} \int_0^\infty \frac{A_1(0)(i\omega_{2c}-x)(\omega_c-ix) - i\beta^{3/2}[A_1(0)-A_2(0)](\sqrt{\omega_c+i\sqrt{-ix}})}{(x-i\omega_{1c})(x-i\omega_{2c})(\omega_c-ix) + i\beta^{3/2}(2x-i\omega_{1c}-\omega_{2c})(\sqrt{\omega_c+i\sqrt{-ix}})} e^{-xt} dx \end{aligned} \quad (\text{B.3})$$

Note that here  $x_j^{(1)}$  are the roots of  $G(x) = 0$  in the region  $\text{Im}(x) < \omega_{1c}$  and  $\text{Re}(x) < 0$

see equation (B.3) above

where  $x_j^{(2)}$  are the roots of  $H(x) = 0$ , and satisfy  $\text{Im}(x_j^{(2)}) < \omega_{1c}$  and  $\text{Re}(x_j^{(2)}) < 0$ .

Substituting equations (B.2, B.3) into equation (B.1), we have

$$\begin{aligned} A_1(t) &= \sum_j \frac{f_1(x_j^{(1)})}{G'(x_j^{(1)})} e^{x_j^{(1)}t} + \sum_j \frac{f_1(x_j^{(2)})}{H'(x_j^{(2)})} e^{x_j^{(2)}t} \\ &\quad - \frac{e^{i\omega_{1c}t}}{\pi i} \int_0^\infty \frac{K_1(x)}{R_1(x) + R_2(x)} e^{-xt} dx. \end{aligned} \quad (\text{B.4})$$

In equation (B.4),  $x_j^{(1)}$  are the roots of  $G(x) = 0$  in the region  $\text{Im}(x_j^{(1)}) > \omega_{1c}$  or  $\text{Re}(x_j^{(1)}) > 0$ ;  $x_j^{(2)}$  are the roots of  $H(x) = 0$  in the region  $\text{Im}(x_j^{(2)}) < \omega_{1c}$  and  $\text{Re}(x_j^{(2)}) < 0$ .

Similarly,  $A_2(t)$  takes the following form:

$$\begin{aligned} A_2(t) &= e^{-i\omega_{12}t} \left[ \sum_j \frac{f_2(x_j^{(1)})}{G'(x_j^{(1)})} e^{x_j^{(1)}t} + \sum_j \frac{f_2(x_j^{(2)})}{H'(x_j^{(2)})} e^{x_j^{(2)}t} \right] \\ &\quad - \frac{e^{i\omega_{2c}t}}{\pi i} \int_0^\infty \frac{K_2(x)}{R_1(x) + R_2(x)} e^{-xt} dx. \end{aligned} \quad (\text{B.5})$$

From equations (4), we can get

$$\begin{aligned} \frac{\partial B_k(t)}{\partial t} &= g_k A_1(t) e^{i(\omega_k - \omega_1)t} + g_k A_2(t) e^{i(\omega_k - \omega_2)t} \\ &= g_k e^{i(\omega_k - \omega_1)t} \left[ \sum_j \frac{f_3(x_j^{(1)})}{G'(x_j^{(1)})} e^{x_j^{(1)}t} + \sum_j \frac{f_3(x_j^{(2)})}{H'(x_j^{(2)})} e^{x_j^{(2)}t} \right] \\ &\quad - \frac{g_k e^{i(\omega_k - \omega_c)t}}{\pi i} \int_0^\infty \left[ \frac{K_1(x) + K_2(x)}{R_1(x) + R_2(x)} \right] e^{-xt} dx. \end{aligned} \quad (\text{B.6})$$

Therefore,

$$\begin{aligned} B_k(t) &= g_k \sum_j \left( \frac{f_3(x_j^{(1)})}{G'(x_j^{(1)})} \frac{e^{i(\omega_k - \omega_1)t + x_j^{(1)}t} - 1}{i(\omega_k - \omega_1) + x_j^{(1)}} \right) \\ &\quad + g_k \sum_j \left( \frac{f_3(x_j^{(2)})}{H'(x_j^{(2)})} \frac{e^{i(\omega_k - \omega_1)t + x_j^{(2)}t} - 1}{i(\omega_k - \omega_1) + x_j^{(2)}} \right) \\ &\quad - \frac{g_k}{\pi i} \int_0^\infty \frac{e^{i(\omega_k - \omega_c)t - xt} - 1}{i(\omega_k - \omega_c) - x} \left[ \frac{K_1(x) + K_2(x)}{R_1(x) + R_2(x)} \right] dx. \end{aligned} \quad (\text{B.7})$$

## Appendix C: The proof of the pure imaginary roots of $\mathbf{G}(\mathbf{s}) = \mathbf{0}$

We now discuss the pure imaginary roots of the following equation and their ranges

$$s(s - i\omega_{12}) - \frac{(2s - i\omega_{12})i\beta^{3/2}}{\sqrt{\omega_c} + \sqrt{-is - \omega_{1c}}} = 0. \quad (\text{C.1})$$

If we set  $s/\beta = ix$  ( $x$  is a real number), and  $\omega_{12}/\beta = \Omega_{12} > 0$ ,  $\omega_{1c}/\beta = \Omega_{1c}$ ,  $\omega_c/\beta = \Omega_c$ , the above equation becomes:

$$-x(x - \Omega_{12}) + \frac{2x - \Omega_{12}}{\sqrt{\Omega_c} + \sqrt{x - \Omega_{1c}}} = 0. \quad (\text{C.2})$$

Obviously, if there are real roots for equation (C.2), the roots are at least in the ranges  $x > \Omega_{1c}$ .

For convenience, we define the following functions,

$$\begin{aligned} y_1 &= -x(x - \Omega_{12}), \quad y_2 = x - \frac{\Omega_{12}}{2}, \\ y_3 &= \frac{2}{\sqrt{\Omega_c} + \sqrt{x - \Omega_{1c}}}, \\ Y &= y_1 + y_2 y_3 = -x(x - \Omega_{12}) + \frac{2x - \Omega_{12}}{\sqrt{\Omega_c} + \sqrt{x - \Omega_{1c}}}, \\ Y' &= -2x + \Omega_{12} + \frac{2}{\sqrt{\Omega_c} + \sqrt{x - \Omega_{1c}}} \\ &\quad - \frac{2x - \Omega_{12}}{2(\sqrt{\Omega_c} + \sqrt{x - \Omega_{1c}})^2 \sqrt{x - \Omega_{1c}}}. \end{aligned}$$

Then the equation (C.2) reduced to  $Y = 0$ .

### C.1 $\Omega_{1c} < 0$

- i. When  $x$  is in the range  $(\Omega_{1c}, 0)$ ,  $y_1 < 0$ ,  $y_2 y_3 < 0$ , we can find  $Y < 0$ , and there is no real root of the equation  $Y = 0$ .
- ii. When  $x$  is in the range  $[0, \Omega_{12}/2]$ , we can find  $Y' > 0$ ,  $Y|_{x=0} < 0$ ,  $Y|_{x=\Omega_{12}/2} = \Omega_{12}^2/4 > 0$ , and there is a real root.
- iii. When  $x$  is in the range  $(\Omega_{12}/2, \Omega_{12})$ , we can find  $Y > 0$ , and there is no real root.
- iv. Finally, we consider the range  $x \in [\Omega_{12}, \infty)$ . Suppose that the root of the equation  $y_2 = y_3$  is  $x_0$ . If  $x_0 \in [\Omega_{12}/2, \Omega_{12}]$ , it is easily verified that

$$Y' < (-2\Omega_{12} + \Omega_{12}) + (\Omega_{12} - \frac{\Omega_{12}}{2}) - 0 = -\frac{\Omega_{12}}{2} < 0,$$

$Y|_{x=\Omega_{12}} > 0$ ,  $Y|_{x \rightarrow \infty} < 0$ . and that there is a real root. If  $x_0 \in (\Omega_{12}, \infty)$ , we see that

$$Y > -x(x - \Omega_{12}) + (x - \frac{\Omega_{12}}{2})^2 = \frac{\Omega_{12}^2}{4} > 0$$

for  $x \in (\Omega_{12}, x_0)$ ,

$$Y' < -2x + \Omega_{12} + (x - \frac{\Omega_{12}}{2}) - 0 = -x + \frac{\Omega_{12}}{2} < 0$$

for  $x \in [x_0, \infty)$ ,

$$Y|_{x=x_0} > -x_0(x_0 - \Omega_{12}) + (x_0 - \frac{\Omega_{12}}{2})^2 = \frac{\Omega_{12}^2}{4} > 0,$$

$Y|_{x \rightarrow \infty} < 0$ , and that there is a real root.

In brief, when  $\Omega_{1c} < 0$ , equation (C.2) has two and only two real roots, which are in the ranges  $(0, \Omega_{12}/2)$  and  $(\Omega_{12}, \infty)$ , respectively.

### C.2 $0 \leq \Omega_{1c} < \Omega_{12}/2$

- i. When  $x \in (\Omega_{1c}, \Omega_{12}/2)$ , we have  $Y' > 0$ ,  $Y|_{x=\Omega_{12}/2} = \Omega_{12}^2/4 > 0$ . Hence, if  $Y|_{x=\Omega_{1c}} < 0$ , a real root exists in this range, if  $Y|_{x=\Omega_{1c}} > 0$ , there is not a real root in this range. This depends on  $\Omega_{1c}$ . If we set  $x = \Omega_{1c}$ , we have

$$-\Omega_{1c}(\Omega_{1c} - \Omega_{12}) + \frac{2\Omega_{1c} - \Omega_{12}}{\sqrt{\Omega_c}} = 0. \quad (C.3)$$

We can also find the roots of equation (C.3):

$$\Omega_{1c}^a = \left( \frac{\Omega_{12}}{2} + \frac{1}{\sqrt{\Omega_c}} \right) - \sqrt{\left( \frac{\Omega_{12}}{2} \right)^2 + \frac{1}{\Omega_c}},$$

$$\Omega_{1c}^b = \left( \frac{\Omega_{12}}{2} + \frac{1}{\sqrt{\Omega_c}} \right) + \sqrt{\left( \frac{\Omega_{12}}{2} \right)^2 + \frac{1}{\Omega_c}}$$

where  $0 < \Omega_{1c}^a < \Omega_{12}/2 < \Omega_{1c}^b$ . That is to say, when  $\Omega_{1c} = \Omega_{1c}^a$  or  $\Omega_{1c} = \Omega_{1c}^b$ ,  $Y|_{x=\Omega_{1c}} = 0$ , *i.e.*, when  $x = \Omega_{1c}^a$  or  $x = \Omega_{1c}^b$ ,  $Y = 0$ . Here we will not consider  $\Omega_{1c}^b$  because  $\Omega_{1c}^b > \Omega_{12}/2$ . We can see when  $x$  is in the range  $(\Omega_{1c}, \Omega_{12}/2]$ ,  $Y' > 0$ ,  $Y|_{x=\Omega_{1c}^a} = 0$  and  $0 < \Omega_{1c}^a < \Omega_{12}/2$ . Hence when  $\Omega_{1c} \in [0, \Omega_{1c}^a]$ ,  $Y|_{x=\Omega_{1c}} < 0$ , a real root exists in the range  $x \in (\Omega_{1c}, \Omega_{12}/2)$ . When  $\Omega_{1c} \in (\Omega_{1c}^a, \Omega_{12}/2)$ ,  $Y|_{x=\Omega_{1c}} > 0$ , there is not a real root in this range.

- ii. When  $x \in (\Omega_{12}/2, \Omega_{12})$ , we have  $Y > 0$ . Hence, no real root exists in this range.  
iii. When  $x \in [\Omega_{12}, \infty)$ , we can easily find that a real root exists, using the same manner in C.1 (iv).

In brief, when  $0 \leq \Omega_{1c} \leq \Omega_{1c}^a$ , two real roots of equation (C.2) exist, and lie in the ranges  $(\Omega_{1c}, \Omega_{12}/2]$  and  $(\Omega_{12}, \infty)$ , respectively. When  $\Omega_{1c}^a < \Omega_{1c} < \Omega_{12}/2$ , there is only one root of equation (C.2) in the range  $(\Omega_{12}, \infty)$ .

### C.3 $\Omega_{12}/2 \leq \Omega_{1c} \leq \Omega_{12}$

- i. Obviously,  $Y > 0$  for  $x \in (\Omega_{1c}, \Omega_{12}]$ , there is no real root in this region.  
ii. For  $x \in (\Omega_{12}, \infty)$ , when  $\Omega_{12}/2 \leq \Omega_{1c} \leq \Omega_{12}/2 + 2/\sqrt{\Omega_c}$ , the root of the equation  $y_2 = y_3$  exists, we can know there is a root of equation (C.2) in the range  $(\Omega_{12}, \infty)$  in the similar way as C.1 (iv). When

$$\Omega_{12}/2 + 2/\sqrt{\Omega_c} < \Omega_{1c} \leq \Omega_{12},$$

there is no root of the equation  $y_2 = y_3$  and  $y_2 > y_3$ . Now,  $Y' < 0$  and  $Y|_{x=\Omega_{12}} > 0$ ,

$$Y|_{x \rightarrow \infty} = -\infty(\infty - \Omega_{12}) + \frac{2\infty - \Omega_{12}}{\sqrt{\Omega_c} + \sqrt{\infty - \Omega_{1c}}} \rightarrow -\infty,$$

*i.e.*,  $Y|_{x \rightarrow \infty} < 0$ . So there is a root of equation (C.2) in the range  $(\Omega_{12}, \infty)$ .

In brief, when  $\Omega_{12}/2 \leq \Omega_{1c} \leq \Omega_{12}$ , equation (C.2) has only one real root in the range  $(\Omega_{12}, \infty)$ .

### C.4 $\Omega_{1c} > \Omega_{12}$

For  $x > \Omega_{1c}$ :

- i. When  $\Omega_{1c} \leq \Omega_{12}/2 + 2/\sqrt{\Omega_c}$ , suppose  $x_0$  is the root of  $y_2 = y_3$ . In the range  $x \in (\Omega_{1c}, x_0]$ ,

$$Y > -x(x - \Omega_{12}) + (x - \Omega_{12}/2)^2 > 0,$$

and no real root exist. But in the range  $x \in (x_0, \infty)$ ,

$$Y' < \Omega_{12} - 2x + (x - \Omega_{12}/2) - 0 = \Omega_{12}/2 - x < 0,$$

$Y|_{x=x_0} = \Omega_{12}^2/4 > 0$ ,  $Y|_{x \rightarrow \infty} < 0$ , and a real root exists.

- ii. When  $\Omega_{1c} > \Omega_{12}/2 + 2/\sqrt{\Omega_c}$ ,  $y_2 > y_3$ ,  $Y' < 0$ , and  $Y|_{x \rightarrow \infty} < 0$ . Now if  $Y|_{x=\Omega_{1c}} > 0$ , there is a real root, and if  $Y|_{x=\Omega_{1c}} < 0$ , no real root exists. In the same way in C.2 (i).  $\Omega_{1c}^a < \Omega_{12}/2 + 2/\sqrt{\Omega_c}$  and  $\Omega_{1c}^b > \Omega_{12}/2 + 2/\sqrt{\Omega_c}$ . So we will only consider  $\Omega_{1c}^a$ . For  $\Omega_{1c} > \Omega_{12}/2 + 2/\sqrt{\Omega_c}$ ,  $Y' < 0$ ,  $Y|_{x=\Omega_{1c}^b} = 0$  and  $\Omega_{1c}^b > \Omega_{12}/2 + 2/\sqrt{\Omega_c}$ . So when  $\Omega_{12} < \Omega_{1c} \leq \Omega_{1c}^b$ ,  $Y|_{x=\Omega_{1c}} > 0$ , a real root exists in the range  $x \in (\Omega_{1c}, \infty)$ . When  $\Omega_{1c} > \Omega_{1c}^b$ ,  $Y|_{x=\Omega_{1c}} < 0$ , no real root exists in the range  $x \in (\Omega_{1c}, \infty)$ .

In brief, when  $\Omega_{12} < \Omega_{1c} \leq \Omega_{1c}^b$ , a real root exists in the range  $(\Omega_{1c}, \infty)$ . When  $\Omega_{1c} > \Omega_{1c}^b$ , no real root exists in this range.

In summary, we have the results:

- (1) when  $\Omega_{1c}^a < \Omega_{1c} \leq \Omega_{1c}^b$ , there is only one root of the equation  $Y = 0$ , which is in the range  $(\max(\Omega_{12}, \Omega_{1c}), \infty)$ ;
- (2) when  $\Omega_{1c} \leq \Omega_{1c}^a$ , there are two roots of the equation  $Y = 0$ , which are in the ranges  $(\max(0, \Omega_{1c}), \Omega_{12}/2)$  and  $(\Omega_{12}, \infty)$ , respectively.

In other words, when  $\omega_{1c}^a < \omega_{1c} \leq \omega_{1c}^b$ , there is only one pure imaginary root  $ib_1$  of the equation (C.1), and  $b_1 \in (\max(\omega_{12}, \omega_{1c}), \infty)$ ; when  $\omega_{1c} \leq \omega_{12}/2$ , there are two pure imaginary roots  $ib_1$  and  $ib_2$  of the equation (C.1), and  $b_1 \in (\omega_{12}, \infty)$ ,  $b_2 \in (\max(0, \omega_{1c}), \omega_{12}/2)$ .

$$\begin{aligned}
\mathbf{E}_l(\mathbf{r}, t) &= Q \sum_j \frac{f_3(x_j^{(1)})}{G'(x_j^{(1)})} \iiint \frac{e^{i(\omega_k - \omega_1)t + ib_j^{(1)}t} - 1}{i(\omega_k - \omega_1) + ib_j^{(1)}} e^{-i(\omega_k t - \mathbf{q} \cdot \mathbf{r})} d^3 \mathbf{q} = Q \sum_j \frac{f_3(x_j^{(1)})}{G'(x_j^{(1)})} \iiint \frac{e^{-i(\omega_1 - b_j^{(1)})t} - e^{-i\omega_k t}}{i(\omega_k - \omega_1) + ib_j^{(1)}} e^{i\mathbf{q} \cdot \mathbf{r}} d^3 \mathbf{q} \\
&= Q \frac{2\pi}{ir} \sum_j \frac{f_3(x_j^{(1)})}{G'(x_j^{(1)})} \int_0^\infty \frac{e^{-i(\omega_1 - b_j^{(1)})t} - e^{-i\omega_k t}}{i(\omega_k - \omega_1) + ib_j^{(1)}} \left( e^{iqr} - e^{-iqr} \right) q dq \\
&= Q \frac{2\pi}{ir} \sum_j \frac{f_3(x_j^{(1)})}{G'(x_j^{(1)})} \left[ e^{-i(\omega_1 - b_j^{(1)})t} \int_{-\infty}^\infty \frac{q e^{iqr}}{i(\omega_k - \omega_1) + ib_j^{(1)}} dq - \int_{-\infty}^\infty \frac{q e^{-i\omega_k t + iqr}}{i(\omega_k - \omega_1) + ib_j^{(1)}} dq \right] \\
&= Q \frac{2\pi}{ir} \sum_j \frac{f_3(x_j^{(1)})}{G'(x_j^{(1)})} \left[ e^{-i(\omega_1 - b_j^{(1)})t} C_a^{(1)} - C_b^{(1)} \right] \tag{D.4}
\end{aligned}$$

$$C_a^{(1)} = \int_{-\infty}^\infty \frac{q e^{iqr}}{i(\omega_k - \omega_1) + ib_j^{(1)}} dq = \frac{\pi}{A} e^{-\frac{r}{l_j}} \tag{D.5}$$

$$\begin{aligned}
C_b^{(1)} &= \int_{-\infty}^\infty \frac{q e^{-i\omega_k t + iqr}}{i(\omega_k - \omega_1) + ib_j^{(1)}} dq \\
&= \frac{\pi}{A} e^{i(b_j^{(1)} - \omega_1)t - r \sqrt{\frac{b_j^{(1)} - \omega_{1c}}{A}}} \Theta \left( \frac{r}{2At} - \sqrt{\frac{b_j^{(1)} - \omega_{1c}}{A}} \right) - e^{-i\omega_k t + \frac{ir^2}{4At}} \int_{-\infty}^\infty \frac{(\rho e^{\frac{3\pi}{4}i} + \frac{r}{2At}) e^{-At\rho^2} e^{\frac{3\pi}{4}i}}{iA(\rho e^{\frac{3\pi}{4}i} + \frac{r}{2At})^2 - i\omega_{1c} + ib_j^{(1)}} d\rho \tag{D.6}
\end{aligned}$$

## Appendix D: The calculation of the radiated field

The amplitude of the radiated field at a particular space point  $\mathbf{r}$  is

$$\begin{aligned}
\mathbf{E}(\mathbf{r}, t) &= \sum_k \sqrt{\frac{\hbar\omega_k}{2\epsilon_0 V}} e^{-i(\omega_k t - \mathbf{k} \cdot \mathbf{r})} B_k(t) \mathbf{e}_k \\
&= \frac{\omega_1 d_1}{2\epsilon_0 V} \sum_k \frac{B_k(t)}{g_k} e^{-i(\omega_k t - \mathbf{k} \cdot \mathbf{r})} \left( \mathbf{u} - \frac{\mathbf{k}(\mathbf{k} \cdot \mathbf{u})}{\mathbf{k}^2} \right) \\
&= \frac{\omega_1 d_1}{16\pi^3 \epsilon_0} \sum_n e^{i\mathbf{k}_0^n \cdot \mathbf{r}} \left( \mathbf{u} - \frac{\mathbf{k}_0^n (\mathbf{k}_0^n \cdot \mathbf{u})}{(\mathbf{k}_0^n)^2} \right) \\
&\quad \times \iiint \frac{B_k(t)}{g_k} e^{-i(\omega_k t - \mathbf{q} \cdot \mathbf{r})} d^3 \mathbf{q} \tag{D.1}
\end{aligned}$$

where we have used  $\mathbf{q} = \mathbf{k} - \mathbf{k}_0^n$ ,  $d^3 \mathbf{q} = d^3 \mathbf{k}$ , and have replaced the sum by an integral *via*  $\sum_k \rightarrow V/(2\pi)^3 \iiint d^3 \mathbf{k}$ . We defined

$$Q = \frac{\omega_1 d_1}{16\pi^3 \epsilon_0} \sum_n e^{i\mathbf{k}_0^n \cdot \mathbf{r}} \left( \mathbf{u} - \frac{\mathbf{k}_0^n (\mathbf{k}_0^n \cdot \mathbf{u})}{(\mathbf{k}_0^n)^2} \right).$$

We assume that

$$\mathbf{q} = q(\sin \theta \cos \phi, \sin \theta \sin \phi, \cos \theta).$$

and  $\mathbf{r}$  is parallel to  $z$ -axis.

From equation (B.7), we can see that,  $B_k(t)$  is composed of the contributions of the poles and an integral

$$B_k(t) = g_k \left( \sum_j B_j^{(1)} + \sum_j B_j^{(2)} + B^{(3)} \right), \tag{D.2}$$

where

$$B_j^{(1)} = \frac{f_3(x_j^{(1)})}{G'(x_j^{(1)})} \frac{e^{i(\omega_k - \omega_1)t + x_j^{(1)}t} - 1}{i(\omega_k - \omega_1) + x_j^{(1)}},$$

$$B_j^{(2)} = \frac{f_3(x_j^{(2)})}{H'(x_j^{(2)})} \frac{e^{i(\omega_k - \omega_1)t + x_j^{(2)}t} - 1}{i(\omega_k - \omega_1) + x_j^{(2)}},$$

$$B^{(3)} = -\frac{1}{\pi i} \int_0^\infty \left[ \frac{K_1(x) + K_2(x)}{R_1(x) + R_2(x)} \right] \frac{e^{i(\omega_k - \omega_c)t - xt} - 1}{i(\omega_k - \omega_c) - x} dx.$$

In these above formulas,  $x_j^{(1)}$  are the pure imaginary roots, and  $x_j^{(2)}$  are the complex roots.

So the field is

$$\begin{aligned}
\mathbf{E}(\mathbf{r}, t) &= Q \iiint \left( \sum_j B_j^{(1)} + \sum_j B_j^{(2)} + B^{(3)} \right) \\
&\quad \times e^{-i(\omega_k t - \mathbf{q} \cdot \mathbf{r})} d^3 \mathbf{q} = \mathbf{E}_l(\mathbf{r}, t) + \mathbf{E}_p(\mathbf{r}, t) + \mathbf{E}_d(\mathbf{r}, t). \tag{D.3}
\end{aligned}$$

1. For the pure imaginary root  $x_j^{(1)} = ib_j^{(1)}$ , we have  $\omega_1 - b_j^{(1)} < \omega_c$

*see equations (D.4–D.6) above*

where  $l_j = \left( \frac{b_j^{(1)} - \omega_{1c}}{A} \right)^{-1/2}$ .

From equations (D.4–D.6), we can obtain

$$\begin{aligned} \mathbf{E}_l(\mathbf{r}, t) = & Q \frac{2\pi}{ir} \sum_j \frac{f_3(x_j^{(1)})}{G'(x_j^{(1)})} \left[ \frac{\pi}{A} e^{-i(\omega_1 - b_j^{(1)})t - r\sqrt{\frac{b_j^{(1)} - \omega_{1c}}{A}}} \Theta \right. \\ & \left. \times \left( t - \frac{r}{2\sqrt{A(b_j^{(1)} - \omega_{1c})}} \right) + e^{-i\omega_c t + \frac{ir^2}{4At} + \frac{3\pi}{4}i} \int_{-\infty}^{\infty} \frac{(\rho e^{\frac{3\pi}{4}i} + \frac{r}{2At})e^{-At\rho^2}}{iA(\rho e^{\frac{3\pi}{4}i} + \frac{r}{2At})^2 - i\omega_{1c} + ib_j^{(1)}} d\rho \right] \end{aligned} \quad (\text{D.7})$$

where  $\Theta(x)$  is the step function: for  $x \geq 0$ ,  $\Theta(x) = 1$ , and for  $x < 0$ ,  $\Theta(x) = 0$ . The first term represents a localized field at frequency  $\omega_1 - b_j^{(1)}$ . The size of the localized photon mode is  $\left(\frac{b_j^{(1)} - \omega_{1c}}{A}\right)^{-1/2}$ . The second term will be zero as time  $t \rightarrow \infty$ .

2. For the complex root  $x_j^{(2)} = a_j^{(2)} + ib_j^{(2)}$ , we have  $a_j^{(2)} < 0$ ,  $\omega_1 - b_j^{(2)} > \omega_c$ .

$$\begin{aligned} \mathbf{E}_p(\mathbf{r}, t) = & Q \sum_j \frac{f_3(x_j^{(2)})}{H'(x_j^{(2)})} \iiint \frac{e^{[i(\omega_k - \omega_1) + a_j^{(2)} + ib_j^{(2)}]t} - 1}{i(\omega_k - \omega_1) + a_j^{(2)} + ib_j^{(2)}} e^{-i(\omega_k t - \mathbf{q} \cdot \mathbf{r})} d^3\mathbf{q} \\ = & Q \frac{2\pi}{ir} \sum_j \frac{f_3(x_j^{(2)})}{H'(x_j^{(2)})} \int_0^{\infty} \frac{e^{a_j^{(2)}t - i(\omega_1 - b_j^{(2)})t} - e^{-i\omega_k t}}{i(\omega_k - \omega_1) + a_j^{(2)} + ib_j^{(2)}} (e^{iqr} - e^{-iqr}) q dq \\ = & Q \frac{2\pi}{ir} \sum_j \frac{f_3(x_j^{(2)})}{H'(x_j^{(2)})} \left[ \int_{-\infty}^{\infty} \frac{e^{a_j^{(2)}t - i(\omega_1 - b_j^{(2)})t} q e^{iqr} dq}{i(\omega_k - \omega_1) + a_j^{(2)} + ib_j^{(2)}} - \int_{-\infty}^{\infty} \frac{q e^{-i\omega_k t + iqr} dq}{i(\omega_k - \omega_1) + a_j^{(2)} + ib_j^{(2)}} \right] \\ = & Q \frac{2\pi}{ir} \sum_j \frac{f_3(x_j^{(2)})}{H'(x_j^{(2)})} \left[ e^{a_j^{(2)}t - i(\omega_1 - b_j^{(1)})t} C_a^{(2)} - C_b^{(2)} \right] \end{aligned} \quad (\text{D.8})$$

$$C_a^{(2)} = \int_{-\infty}^{\infty} \frac{q e^{iqr}}{i(\omega_k - \omega_1) + a_j^{(2)} + ib_j^{(2)}} dq = \frac{\pi}{A} e^{-ir\sqrt{\frac{\omega_{1c} - b_j^{(2)} + ia_j^{(2)}}{A}}} \quad (\text{D.9})$$

$$\begin{aligned} C_b^{(2)} = & \int_{-\infty}^{\infty} \frac{q e^{-i\omega_k t + iqr}}{i(\omega_k - \omega_1) + a_j^{(2)} + ib_j^{(2)}} dq = e^{-i\omega_c t + \frac{ir^2}{4At}} \int_{-\infty}^{\infty} \frac{(q + \frac{r}{2At})e^{-iAtq^2}}{iA(q + \frac{r}{2At})^2 - i\omega_{1c} + a_j^{(2)} + ib_j^{(2)}} dq \\ = & e^{-i\omega_c t + \frac{ir^2}{4At}} \left[ \int_0^{\infty} + \int_{-\infty}^0 \right] \frac{(q + \frac{r}{2At})e^{-iAtq^2}}{iA(q + \frac{r}{2At})^2 - i\omega_{1c} + a_j^{(2)} + ib_j^{(2)}} dq \\ = & \frac{\pi}{A} e^{(a_j^{(2)} + ib_j^{(2)} - i\omega_1)t - ir\sqrt{\frac{\omega_{1c} - b_j^{(2)} + ia_j^{(2)}}{A}}} - e^{-i\omega_c t + \frac{ir^2}{4At}} \int_{-\infty}^{\infty} \frac{(\rho e^{\frac{3\pi}{4}i} + \frac{r}{2At})e^{-At\rho^2} e^{\frac{3\pi}{4}i}}{iA(\rho e^{\frac{3\pi}{4}i} + \frac{r}{2At})^2 - i\omega_{1c} + a_j^{(2)} + ib_j^{(2)}} d\rho \\ & - \frac{\pi}{A} e^{(a_j^{(2)} + ib_j^{(2)} - i\omega_1)t + ir\sqrt{\frac{\omega_{1c} - b_j^{(2)} + ia_j^{(2)}}{A}}} \Theta \left[ t - \frac{r}{2\sqrt{A}(\text{Re} + \text{Im})\sqrt{\omega_{1c} - b_j^{(2)} + ia_j^{(2)}}} \right]. \end{aligned} \quad (\text{D.10})$$

From equations (D.8–D.10), we can obtain

$$\begin{aligned} \mathbf{E}_p(\mathbf{r}, t) = & Q \frac{2\pi}{ir} \sum_j \frac{f_3(x_j^{(2)})}{H'(x_j^{(2)})} \left\{ \frac{\pi}{A} e^{(a_j^{(2)} + ib_j^{(2)} - i\omega_1)t + ir\sqrt{\frac{\omega_{1c} - b_j^{(2)} + ia_j^{(2)}}{A}}} \Theta \left[ t - \frac{r}{2\sqrt{A}(\text{Re} + \text{Im})\sqrt{\omega_{1c} - b_j^{(2)} + ia_j^{(2)}}} \right] \right. \\ & \left. + e^{-i\omega_c t + \frac{ir^2}{4At} + \frac{3\pi}{4}i} \int_{-\infty}^{\infty} \frac{(\rho e^{\frac{3\pi}{4}i} + \frac{r}{2At})e^{-At\rho^2}}{iA(\rho e^{\frac{3\pi}{4}i} + \frac{r}{2At})^2 - i\omega_{1c} + a_j^{(2)} + ib_j^{(1)}} d\rho \right\}. \end{aligned} \quad (\text{D.11})$$

In the above equation, the second term decays to zero and can be neglected as time  $t \rightarrow \infty$ . The first term is a pulse.

3. Similarly, we can obtain the contribution of  $B^{(3)}$

$$\begin{aligned} \mathbf{E}_d(\mathbf{r}, t) &= -\frac{Q}{2\pi i} \int_0^\infty \left[ \frac{K_1(x) + K_2(x)}{R_1(x) + R_2(x)} \right] dx \iiint \frac{e^{i(\omega_k - \omega_c)t - xt} - 1}{i(\omega_k - \omega_c) - x} e^{-i(\omega_k t - \mathbf{q} \cdot \mathbf{r})} d^3 \mathbf{q} \\ &= \frac{Q}{r} \int_0^\infty \left[ \frac{K_1(x) + K_2(x)}{R_1(x) + R_2(x)} \right] dx \int_0^\infty \frac{e^{-(x+i\omega_c)t} - e^{-i\omega_k t}}{i(\omega_k - \omega_c) - x} (e^{iqr} - e^{-iqr}) q dq \\ &= \frac{Q}{r} \int_0^\infty \left[ \frac{K_1(x) + K_2(x)}{R_1(x) + R_2(x)} \right] dx \left[ e^{-(x+i\omega_c)t} \int_{-\infty}^\infty \frac{qe^{iqr}}{i(\omega_k - \omega_c) - x} dq - \int_{-\infty}^\infty \frac{qe^{-i\omega_k t + iqr}}{i(\omega_k - \omega_c) - x} dq \right] \\ &= \frac{Q}{r} \int_0^\infty \left[ \frac{K_1(x) + K_2(x)}{R_1(x) + R_2(x)} \right] dx \left[ e^{-(x+i\omega_c)t} C_a^{(3)} - C_b^{(3)} \right] \end{aligned} \quad (\text{D.12})$$

$$C_a^{(3)} = \int_{-\infty}^\infty \frac{qe^{iqr}}{i(\omega_k - \omega_c) - x} dq = \frac{\pi}{A} e^{-\sqrt{i} \sqrt{\frac{x}{A}} r} \quad (\text{D.13})$$

$$\begin{aligned} C_b^{(3)} &= \int_{-\infty}^\infty \frac{qe^{-i\omega_k t + iqr}}{i(\omega_k - \omega_c) - x} dq = e^{-i\omega_c t + \frac{ir^2}{4At}} \int_{-\infty}^\infty \frac{(q + \frac{r}{2At})e^{-iAtq^2}}{iA(q + \frac{r}{2At})^2 - x} dq = e^{-i\omega_c t + \frac{ir^2}{4At}} \left[ \int_0^\infty + \int_{-\infty}^0 \right] \frac{(q + \frac{r}{2At})e^{-iAtq^2}}{iA(q + \frac{r}{2At})^2 - x} dq \\ &= \frac{\pi}{A} e^{-xt - i\omega_c t - r\sqrt{i} \sqrt{\frac{x}{A}}} - e^{-i\omega_c t + \frac{ir^2}{4At}} \int_{-\infty}^\infty \frac{(\rho e^{\frac{3\pi}{4}i} + \frac{r}{2At})e^{-At\rho^2} e^{\frac{3\pi}{4}i}}{iA(\rho e^{\frac{3\pi}{4}i} + \frac{r}{2At})^2 - x} d\rho. \end{aligned} \quad (\text{D.14})$$

From equations (D.12–D.14), we can obtain

$$\begin{aligned} \mathbf{E}_d(\mathbf{r}, t) &= \frac{Q}{r} \int_0^\infty \left[ \frac{K_1(x) + K_2(x)}{R_1(x) + R_2(x)} \right] dx e^{-i\omega_c t + \frac{ir^2}{4At}} \int_{-\infty}^\infty \frac{(\rho e^{\frac{3\pi}{4}i} + \frac{r}{2At})e^{-At\rho^2} e^{\frac{3\pi}{4}i}}{iA(\rho e^{\frac{3\pi}{4}i} + \frac{r}{2At})^2 - x} d\rho, \\ &= \frac{Q}{rA} \int_0^\infty \left[ \frac{K_1(x) + K_2(x)}{R_1(x) + R_2(x)} \right] dx e^{-i\omega_c t + \frac{ir^2}{4At}} \int_{-\infty}^\infty \frac{(ye^{\frac{3\pi}{4}i} + \frac{r}{2\sqrt{At}})e^{-y^2} e^{\frac{3\pi}{4}i}}{i(ye^{\frac{3\pi}{4}i} + \frac{r}{2\sqrt{At}})^2 - xt} dy. \end{aligned} \quad (\text{D.15})$$

## References

1. S. John, Phys. Rev. Lett. **53**, 2169 (1984); P.W. Anderson, Philos. Mag. B **52**, 505 (1985).
2. E. Yablonovitch, Phys. Rev. Lett. **58**, 2059 (1987); S. John, *ibid.* **58**, 2486 (1987).
3. E. Yablonovitch, T. Gmitter, Phys. Rev. Lett. **63**, 1950 (1989); K.M. Ho, C.T. Chan, C.M. Soukoulis, *ibid.* **65**, 3152 (1990); E. Yablonovitch, T. Gmitter, K.M. Leung, *ibid.* **67**, 2295 (1991); E. Yablonovitch, J. Opt. Soc. Am. B **10**, 283 (1993); G. Kweon, N.M. Lawandy, J. Mod. Opt. **41**, 311 (1994); U. Grünig, V. Lehmann, C.M. Engelhart, Appl. Phys. Lett. **66**, 3254 (1995); J.D. Joannopoulos, R.D. Meade, J.N. Winn, *Photonic Crystals* (Princeton, New York, 1995); I.I. Tarhan, G.H. Watson, Phys. Rev. Lett. **76**, 315 (1996).
4. S. John, J. Wang, Phys. Rev. Lett. **64**, 2418 (1990); Phys. Rev. B **43**, 12772 (1991).
5. S. John, T. Quang, Phys. Rev. A **50**, 1764 (1994).
6. S. John, T. Quang, Phys. Rev. Lett. **74**, 3419 (1995); *ibid.* **76**, 1320 (1996); *ibid.* **78**, 1888 (1997);
7. S. Bay, P. Lambropoulos, K. Molmer, Opt. Commun. **132**, 237 (1996); Phys. Rev. A **55**, 1485 (1997); Phys. Rev. Lett. **79**, 2654 (1997); S. Bay, P. Lambropoulos, Opt. Commun. **146**, 130 (1998).
8. S.-y. Zhu, H. Chen, H. Huang, Phys. Rev. Lett. **79**, 205 (1997); Y.-p. Yang, S.-y. Zhu, M.S. Zubairy, Opt. Commun. **79**, 166 (1999); S.Y. Xie, Y.-p. Yang, H. Chen, S.-y. Zhu, X. Wu, Chin. Phys. Lett. **17**, 25 (2000); H. Hang, X.H. Lu, S.-y. Zhu, Phys. Rev. **57**, 4945 (1998).
9. E. Yablonovitch, J. Opt. Soc. Am. B **10**, 283 (1993).
10. T. Quang, M. Woldeyohannes, S. John, G.S. Agarwal, Phys. Rev. Lett. **79**, 5238 (1997).
11. S.-y. Zhu, Y.-p. Yang, H. Chen, H. Zheng, M.S. Zubairy, Phys. Rev. Lett. **84**, 2136 (2000).
12. M.O. Scully, M.S. Zubairy, *Quantum Optics* (Cambridge University Press, Cambridge, England, 1997), Chap. 10.